

ABSTRACT

Title of Document: HYBRID FREE-SPACE AND RADIO
FREQUENCY SWITCHING

David Storm Kim
Master of Science, 2008

Directed By: Professor Isaak Mayergoyz
Department of Electrical and Computer
Engineering

The characterization and switching system for a hybrid Free-Space Optical (FSO) with Radio Frequency (RF) backup link is described. Such hybrid systems are used to take advantage of the large bit rates achieved with FSO while maintaining high reliability with a RF backup. In this project, monitoring and switching are controlled by a program that checks the FSO connection health using echo packets. The switching program was tested using a fiber optic link that can simulate atmospheric attenuation effects, such as scintillation, by using an optical modulator. The system's sensitivity to connection quality degradation and momentary connection outages can be optimized for a given situation. The simplicity and ease of implementation are the main strong points of this system.

HYBRID FREE-SPACE AND RADIO FREQUENCY SWITCHING

By

David Storm Kim

Thesis submitted to the Faculty of the Graduate School of the
University of Maryland, College Park, in partial fulfillment
of the requirements for the degree of
Master of Science
2008

Advisory Committee:
Professor Isaak Mayergoyz, Chair
Professor Thomas Murphy
Professor Christopher Davis

© Copyright by
David Storm Kim
2008

Acknowledgements

I would like to thank my supervisor Dr. G. Charmaine Gilbreath at the Naval Research Lab. Without her support this project would not have been possible. I would like to also thank Jonathan Doffoh for providing technical assistance and guidance and the initial equipment needed to get the project started. Also I am grateful for the support and assistance that the rest of Code 5505 provided for me during all my hours in the lab.

I would also like to extend my gratitude to my advisor, Professor Isaak Mayergoyz, for taking the time to meet with and give advice to me whenever I needed it during my graduate career. Also thanks to Professor Thomas Murphy and Professor Christopher Davis for generously donating their time to sit on my committee.

Table of Contents

Acknowledgements.....	ii
Table of Contents.....	iii
List of Figures.....	iv
Chapter 1: Introduction.....	1
1.1 Free-Space Optical Availability.....	1
1.2 Hybrid System Availability.....	3
1.3 Objective.....	4
Chapter 2: Atmospheric Channel Effects.....	5
2.1 Absorption.....	5
2.2 Scattering.....	7
2.2.1 Rayleigh Scattering.....	7
2.2.2 Mie Scattering.....	9
2.3 Turbulence and Scintillation.....	10
Chapter 3: Hybrid RF/FSO Utilization Schemes.....	14
3.1 Network Architecture.....	14
3.2 Switching Method.....	15
3.3 Coding Method.....	17
Chapter 4: Experimental Setup.....	20
4.1 Setup.....	20
4.1.1 Modulator.....	24
4.1.2 Media Converters.....	27
4.2 Scintillation Data and Switching Program.....	31
Chapter 5: Data and Results.....	34
5.1 Initial Performance Measurements.....	34
5.1.1 MGEN Data.....	34
5.1.2 Echo Packet Losses.....	41
5.2 Switching Performance.....	43
5.2.1 Scintillation Affected Switching.....	43
5.2.2 Line of Sight Blocking.....	49
Chapter 6: Conclusion.....	55
Appendix A- Transmission and Loss Graphs for 100, 90, and 80 nW.....	58
Appendix B- Matlab Code for Scintillation Data Formatting.....	60
Appendix C- C++ Code for Switching Program.....	61
Bibliography.....	68

List of Figures

Figure 2-1 Transmittance of light through the atmosphere	6
Figure 2-2 Aperture averaging factor vs. receiver diameter	12
Figure 4-1 RF/Optic link configuration	21
Figure 4-2 RF modem and routers	21
Figure 4-3 Network map	22
Figure 4-4 Attenuator and modulator	23
Figure 4-5 Mach-Zehnder modulator layout	25
Figure 4-6 Transmission curve for modulator	26
Figure 4-7 MiniMc Media Converters	27
Figure 4-8 Transmission and loss for 130 nW	28
Figure 4-9 Transmission and loss for 120 nW	29
Figure 4-10 Transmission and loss for 110 nW	30
Figure 4-11 Transmission and loss for 70 nW	31
Figure 4-12 Formatted scintillation data	32
Figure 5-1 Transmission rate for minimal degradation of link quality	34
Figure 5-2 Packet loss for minimal degradation of link quality	35
Figure 5-3 Transmission rate for increased fade	36
Figure 5-4 Packet loss for increased fade	36
Figure 5-5 Transmission rate for maximum fade	37
Figure 5-6 Packet loss for maximum fade	37
Figure 5-7 Transmission rate for greater scintillation	38
Figure 5-8 Packet loss for greater scintillation	39

Figure 5-9 Transmission rate for greatest level of scintillation	40
Figure 5-10 Packet loss for greatest level of scintillation	40
Figure 5-11 Echo packet loss for 5-100 second averaging intervals	41
Figure 5-12 Transmission rate for 50 second averaging window	43
Figure 5-13 Packet loss for 50 second averaging window	44
Figure 5-14 Transmission rate for 25 second averaging window	45
Figure 5-15 Packet loss for 25 second averaging window	45
Figure 5-16 Transmission rate for 10 second averaging window	46
Figure 5-17 Packet loss for 10 second averaging window	47
Figure 5-18 Transmission rate for 5 second averaging window	48
Figure 5-19 Packet loss for 5 second averaging window	48
Figure 5-20 Line of sight block test for 50 second window	50
Figure 5-21 Line of sight block test for 25 second window	51
Figure 5-22 Line of sight block test for 10 second window	52
Figure 5-23 Line of sight block test for 5 second window	53

Chapter 1: Introduction

Free-Space Optical (FSO) communication technology has developed and matured greatly over recent years. The advantages it has over traditional Radio Frequency (RF) communication, such as high data rates, low power consumption, license-free spectrum, has made it a topic of high interest [1, 2]. FSO is well suited for point-to-point communication where high bandwidth and security are a concern [3]. It can also be integrated with existing fiber optic backbones to provide ‘last mile access’ solutions where laying down fiber lines is too expensive or impractical [4, 5]. However, the main disadvantage of FSO is its greater susceptibility to atmospheric weather conditions for link quality. Atmospheric effects such as absorption, scattering, and scintillation all work to degrade FSO link quality [6]. In general, this makes FSO less reliable than RF communications and therefore one solution that has been devised is to supplement an FSO link with an RF or Millimeter Wave (MMW) link for greater reliability [7].

1.1 Free-Space Optical Availability

The main obstacle to greater widespread use of FSO is link availability. For carrier class applications, availability of 99.999% (or “5 nines”) is typically required, which corresponds to about 5 minutes of downtime a year. FSO alone is not usually able to achieve this unless link ranges are generally less than 140 m. This is due to the unpredictable nature of atmospheric attenuation on laser beams. Typically, single mode optical fibers have attenuation losses of less than 0.5 dB/km. This loss is constant and can be accommodated for, in communication link designs. On the other

hand, atmospheric attenuation is quite variable with losses of anywhere between 0.2 dB/km to 350 dB/km. This makes FSO links highly variable and unpredictable, usually making 99.999% availability difficult if not impossible for FSO links across any significant distance.

One would normally think to increase the transmit power to increase range. However, this does not produce significant increases in link range particularly within dense fog. For example, if one were to try transmitting at the highest conceivable power of about 10 W, which would be above the eye safe limit of 100 mW/cm² at 1550 nm for a 4 inch diameter transmit aperture, and having the lowest conceivable receive power of about 1 nW, for a data rate of 100 Mbps. Also, consider that this system uses an unrealistically perfect telescope system that couples all the transmitted power to the receiver at the other end. This system would have an amazing 100 dB of margin for atmospheric attenuation, compared to about 50 dB margin for a typical FSO system. Even with this margin, in the heaviest fog with about 350 dB/km attenuation, the link range could only be extended to 286 m.

It is apparent that increasing the power of an FSO link is not a viable solution to weather related link loss. The most cost-effective means to increase availability is by using an RF or MMW back-up link. Both of which would not be affected by the same attenuating weather conditions. Although the bandwidth of RF systems is much lower than FSO, the percentage of time the RF will be used as the primary link will be small compared to the larger bandwidth FSO. The added link will allow for 99.999% availability over longer ranges than FSO alone [8].

1.2 Hybrid System Availability

FSO and RF or MMW links have better availability than FSO only links due to the fact that RF and MMW are not as affected by fog, which is FSO's largest limiting factor. Heavy fog can attenuate FSO anywhere from 100-350 dB/km [8]. Whereas MMW attenuation for moderate to heavy fog, for 60 GHz, range from 0.1-1 dB/km [9]. On the other hand, rain affects MMW and FSO similarly but more than RF. For MMW frequencies between 30-60 GHz, heavy rain (60 mm/hr) can attenuate between 15-22 dB/km depending on frequency [10]. FSO can be attenuated by about 16 dB/km for 60 mm/hr rainfall [3]. But for RF, attenuation for frequencies below 10 GHz are negligible [11]. Although the data rate for RF may be lower than MMW, in areas of heavy and frequent rain RF would be the better option for greater availability, since FSO/MMW systems would be similarly susceptible to attenuation effects of rain.

For example in Malaysia, a region with frequent rains, the average rain intensity exceeding 0.01% of the year is 120 mm/hr, which attenuates FSO power by 28 dB/km. For 99.99% availability, the link would be limited to 800 m if it is a FSO only system and even shorter for 99.999% availability [3]. If an RF link is added as backup, 99.999% availability could be maintained for ranges greater than 800 m. Although the trade off will be that the percentage of time the lower bandwidth RF link will be active will increase due to the more frequent loss of the FSO link.

1.3 Objective

In this project, the goal of designing and testing a simple system to perform switching between RF and optical links in a hybrid system was set. To accomplish this, all switching and monitoring tasks are designed to be performed in software with no use of specialized hardware other than what is widely available and off the shelf. In order to simplify testing, instead of an actual FSO setup a fiber optic link was used to simulate an FSO link. This was done by using an optical modulator as the main generator for simulated atmospheric attenuation. A simple monitoring scheme using echo packets is described in this experiment and the results of switching based on this design is presented.

Chapter 2: Atmospheric Channel Effects

In FSO communications, the atmosphere is the greatest limiting factor when transmitting light over appreciable distances. Effects from fog, rain, and snow can lower data throughput or even break the communication link all together. Even on clear days, atmospheric scattering and turbulence can affect proper transmission. This turbulence causes what's known as scintillation of the laser beam.

Some of these effects are well known and have good models for prediction. Effects such as absorption and scattering are well understood and their effect can be accurately predicted given known environmental conditions. On the other hand, scintillation from turbulence is essentially a random effect and therefore very difficult to anticipate let alone predict.

2.1 Absorption

The atmosphere is composed of various gas molecules. Absorption occurs when a photon is absorbed by a gas molecule and the energy of the photon is converted into kinetic energy. Essentially, this is a mechanism by which the atmosphere is heated [12]. The molecules are characterized by their index of refraction. An important quantity for absorption and scattering is the extinction coefficient, α . The imaginary part of the index of refraction, k , is related to the extinction coefficient by the following:

$$\alpha = \frac{4\pi k}{\lambda} = \sigma N \quad (2.1)$$

Where σ is the extinction cross section and N is the concentration of molecules or particles. This absorption is highly dependent on wavelength, λ [13]. For example, absorption by O_2 and O_3 essentially block all transmission for wavelengths below 200 nm [12]. In the near IR range, absorption is mainly due to water vapor and at higher wavelengths CO_n and NO_n absorption become more important [14]. For wavelengths available for use in FSO, 0.7-10 μm , lasers can be selected in windows of transmittance to avoid most of the absorption. These windows of transmittance can be seen in Figure 2-1.

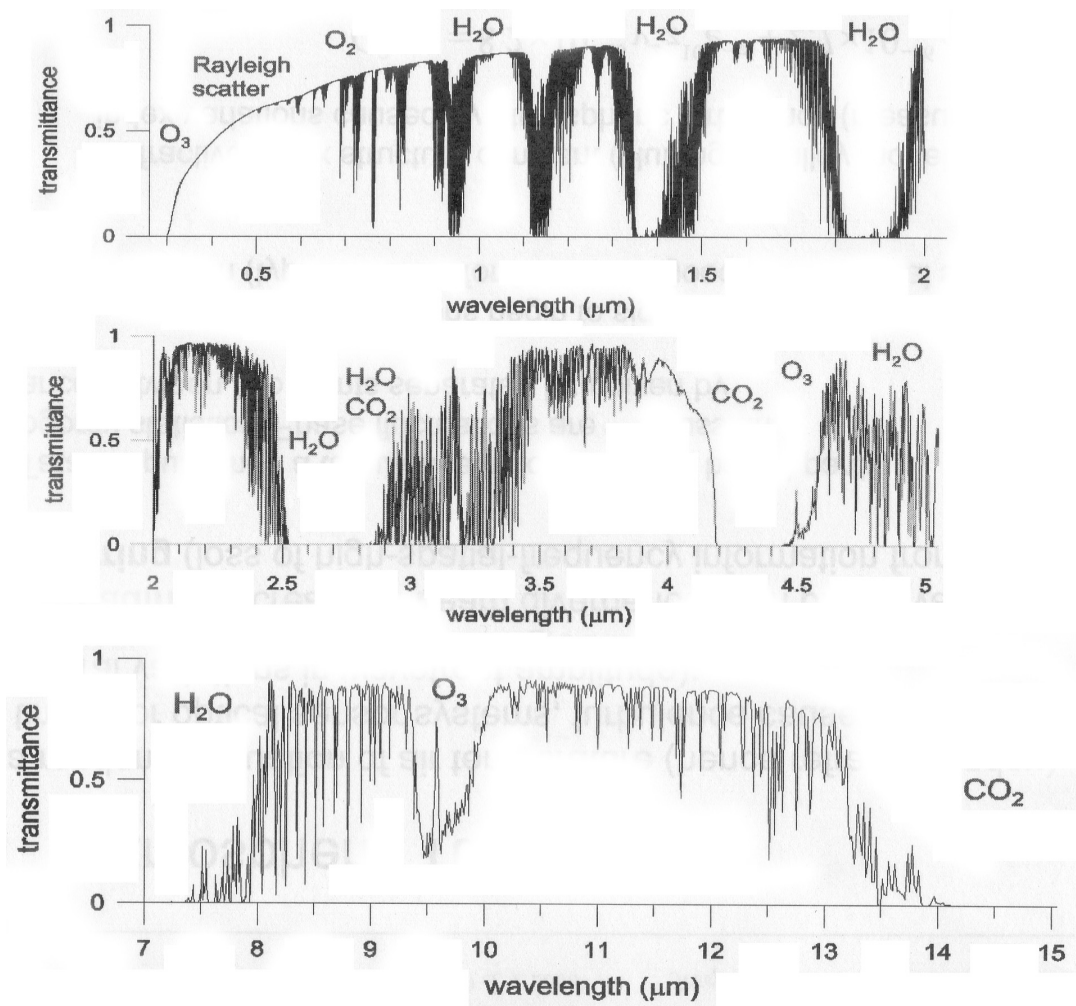


Figure 2-1. Transmittance of light through the atmosphere [15].

Typically, commercial FSO systems operate in windows around 850 nm and 1550 nm. Since these wavelengths are also used in fiber optic communications, standard components can be used lowering cost. There are other transmission windows available in the ranges between 3-5 μm and 8-14 μm , but the availability of components in these wavelengths are limited and more expensive [13].

2.2 Scattering

Scattering is the process by which radiation, such as light, is redirected from its straight-line path. The two main kinds of scattering in the atmosphere are Rayleigh and Mie. They are both elastic forms of scattering but Rayleigh occurs for particle diameters much less than the wavelength of incident light and Mie occurs for diameters comparable to the wavelength of light. Air molecules are the main source of scattering for Rayleigh and larger dust particles and water droplets, such as fog, are the main source of scattering for Mie [16].

2.2.1 Rayleigh Scattering

Rayleigh scattering is caused by the elastic scattering of electromagnetic radiation which occurs when the electric field of photons interact with the electric field of gas molecules. The elastic nature of the interaction means that there is no net exchange of energy between the photon and gas molecule. Therefore the scattered photon has the same wavelength as the original incident photon [17]. The light is also equally scattered in the forward and backward directions. For Rayleigh scattering to occur, the particle diameter should be much smaller than the wavelength of incident

light [18]. At wavelengths below 1 μm , Rayleigh scattering is quite strong while wavelengths greater than 3 μm experience almost no scattering.

An important quantity in Rayleigh scattering, as in absorption, is the extinction coefficient. This is a measure of the fractional loss of light per unit distance due to scattering and absorption.

$$\alpha(\lambda) = A_a + S_a \quad (2.2)$$

The extinction coefficient has both absorption and scattering components, where A_a is the absorption coefficient and S_a is the scattering coefficient. The coefficients are a function of incident light wavelength and dependent on what's known as the extinction cross section of the molecule or particle [12]. The extinction cross section is shown as:

$$\sigma \approx \frac{2k^4}{3\pi N^2} |n - 1|^2 \quad (2.3)$$

Where k is the wave number, N is the number of molecules per unit volume, and n the index of refraction, assuming $|n - 1| \ll 1$. The extinction coefficient can be rewritten in terms of the extinction cross section as:

$$\alpha = N\sigma \approx \frac{2k^4}{3\pi N} |n - 1|^2 \quad (2.4)$$

The k^4 dependence shows that higher frequencies are scattered much more, which is what gives the sky its blue color since the shorter wavelengths are scattered out from sunlight first [19]. The transmittance of light through a distance L can be found by using Beer's Law:

$$T = \exp[-\alpha(\lambda)L] \quad (2.5)$$

The product $\alpha(\lambda)L$ is also called the optical depth and describes the amount of extinction (absorption + scattering) that occurs through a medium [12]. For typical wavelengths used in FSO communications, mainly infrared, the effect of Rayleigh scattering is not significant due to the relatively long wavelengths used.

2.2.2 Mie Scattering

For particle sizes comparable to the wavelength of incident light, Rayleigh scattering cannot be used to describe the effects. Instead, Mie scattering must be used. Mie scattering is a complete analytic solution to Maxwell's equations for the scattering of radiation but is only valid for spherical particles. Unlike Rayleigh scattering, Mie scattering favors scattering in the forward direction [18]. There are several models for Mie used to calculate attenuation for optical signals due to scattering from fog. The two most common are the Kim and Kruse model [6]. These models use visibility data to determine the amount of attenuation expected. The specific attenuation for both models is given by:

$$a_{\text{spec}} = \frac{10 \text{Log} V\%}{V(\text{km})} \left(\frac{\lambda}{\lambda_0} \right)^{-q} \text{ (dB/km)} \quad (2.6)$$

Where $V(\text{km})$ is visibility, $V\%$ is the percentage of object contrast to original, λ is wavelength in nm, λ_0 is the visibility reference (550 nm). For the Kruse model:

$$q = \begin{cases} 1.6 & \text{if } V > 50 \text{ km} \\ 1.3 & \text{if } 6 \text{ km} < V < 50 \text{ km} \\ 0.585V^{1/3} & \text{if } V < 6 \text{ km} \end{cases} \quad (2.7)$$

This implies there is less attenuation for higher wavelengths. However, the Kim model rejects wavelength dependence for low visibility in dense fog. The q for the Kim model is given by:

$$q = \begin{cases} 1.6 & \text{if } V > 50 \text{ km} \\ 1.3 & \text{if } 6 \text{ km} < V < 50 \text{ km} \\ 0.16V + 0.34 & \text{if } 1 \text{ km} < V < 6 \text{ km} \\ V - 0.5 & \text{if } 0.5 \text{ km} < V < 1 \text{ km} \\ 0 & \text{if } V < 0.5 \text{ km} \end{cases} \quad (2.8)$$

For visibility less than 500 m, the Kim model shows there is no wavelength dependence for attenuation [20]. This means, unlike with absorption, a particular wavelength cannot be chosen to minimize or eliminate the effects of Mie scattering due to its insensitivity to wavelength at low visibilities.

2.3 Turbulence and Scintillation

Even on clear weather days, light travelling through the atmosphere will experience fluctuations in intensity. This is caused by uneven heating and temperature differences of air cells in the atmosphere. These differences create differences in the index of refraction altering the path light takes through the atmosphere. These air pockets are not stable and cause something called turbulence. Turbulence has three main effects. First is the deflection of the beam due to the randomly changing index of refraction, called beam wander. Second is scintillation, which is the fluctuation in intensity of the beam wave front. Last is the added divergence of the beam.

The radial variance due to beam wander is described by the following equation:

$$\sigma_r = 1.83C_n^2 \lambda^{-1/6} L^{17/6} \quad (2.9)$$

This shows that longer wavelengths, λ , experience less beam wander than shorter wavelengths. Here σ_r is the radial variance, L the distance travelled by the beam, and

C_n^2 is the strength of turbulence [13]. C_n^2 has the units of $m^{-2/3}$ and appears in almost anything that describes turbulence. C_n^2 can range in value from $10^{-15} m^{-2/3}$ to $10^{-18} m^{-2/3}$. The most important variable in its change is the wind and altitude. The higher the altitude, the colder and less dense the air gets, so the turbulence level is lower. In general, there is no accepted average value for C_n^2 since it can vary greatly depending on the time, location, and ground conditions [21].

The next effect of turbulence is scintillation. Of the three effects of turbulence, scintillation may be the most noticeable effect for FSO systems [13]. Light travelling through scintillation will experience intensity fluctuations, even over relatively short propagation paths. Scintillation is almost completely caused by small temperature variations which create fluctuations in the index of refraction [12]. As light propagates through the fluctuations, it is constantly being focused and defocused. This causes a loss of spatial coherence and creates destructive and constructive interference with different parts of the light wave front [21]. This can cause receiver saturation or signal loss. Scintillation effects for small fluctuations follow a log-normal distribution characterized by the variance σ_i given by the following:

$$\sigma_i^2 = 1.23C_n^2 k^{7/6} L^{11/6} \quad (2.10)$$

Here, k is the wave number and this expression suggests that longer wavelengths experience a smaller variance. For large fluctuations, the following equation holds:

$$\sigma_{\text{high}}^2 = 1 + 0.86 (\sigma_i^2)^{-2/5} \quad (2.11)$$

This suggests that for larger fluctuations, the opposite is true, shorter wavelengths experience a smaller variance [13]. Scintillation effects can in part be mitigated by using a larger receiver area in what is known as aperture averaging. However, this is

limited by the practical size and weight a receiver can realistically be made. The ratio of the intensity variance of fluctuations of a receiver with diameter D to a point receiver is known as the aperture averaging factor. This factor tails off beyond a certain size of receiver for a given range and degree of turbulence. An example of this is seen in the figure below [22]:

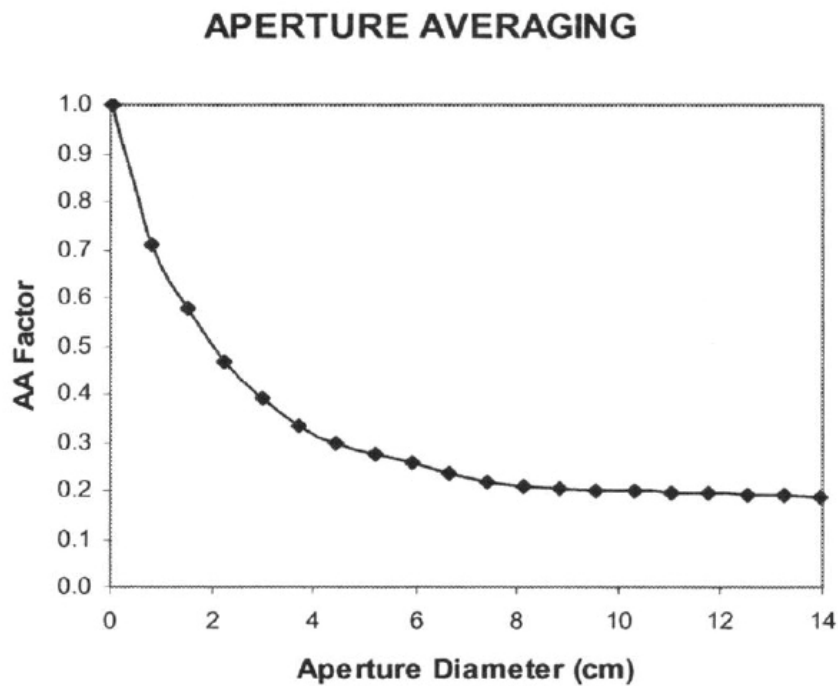


Figure 2-2. Aperture averaging factor vs. receiver diameter [22].

Beyond a certain receiver size there is no significant reduction in the variance. Therefore the variance can only be improved to a set practical limit and scintillation can remain a significant factor depending on the system setup.

Lastly, turbulence also induces beam spreading beyond what would be predicted by diffraction theory alone. In particular for lasers, the intensity profile is usually Gaussian in form. Over a long distance L , the beam waist, w_b , is given as:

$$w_b^2 = \left(\frac{4L^2}{k^2 w_0^2} \right) + 3.58 C_n^2 L^3 w_0^{-1/3} \quad (2.12)$$

Where w_0 is the beam waist at the transmitting aperture and k is the wave number.

This equation shows that the waist grows over long distances because of turbulence, which essentially decreases the power received since there is added dispersion [21].

In essence, turbulence is a random phenomenon and there is no way to know moment to moment how much scintillation a FSO signal will experience. It can cause prolonged or sporadic losses in link quality or connection. But it is essentially an attenuation effect and even though it can introduce phase distortions in the wave front, this is not as significant a factor in communication applications. One only needs to get light into the “bucket” and spatial resolution is usually more important only for optical imaging applications.

Chapter 3: Hybrid RF/FSO Utilization Schemes

In this project, a simple scheme was chosen and tested for hybrid RF/FSO utilization. But it is beneficial to study what other possible methods exist and to evaluate what future improvements can be made after. In choosing and adapting a method, practicality considerations must be made. In general, there is a tradeoff of improved system performance for increased complexity and cost.

3.1 Network Architecture

There are many possible methods that can be used to provide switching in hybrid FSO/RF systems. Some of the key issues that should be considered when selecting a particular method are switching efficiency, latency, ease of design, and implementation.

Networks can be described as an abstract layered model such as the Open Systems Interconnection Basic Reference Model (OSI Model). This model divides network architecture into seven layers with each layer providing a more basic service than the level above it. The lowest layer is the Physical Layer. This layer provides the actual physical hardware and medium in which data is transmitted. Whether it be electrical signals through a wire or light pulses through free space, the Physical Layer provides the encoding, transmission, and decoding of information into and out of the physical medium for the higher layers to process and use. The next layer up is the Data Link Layer. This layer allows for communication between stations on a link. The Data Link Layer takes the bits received from the Physical Layer and arranges them into frames. This layer can also provide error detection and data flow control.

An Ethernet switch is an example of a device that operates at the Data Link Layer. On top of the Data Link Layer is the Network Layer. The Network layer establishes communication between stations across different links and networks. This layer provides a level of independence from the two lower levels and allows for the transfer of variable length data sequences. Routers operate at this level and usually make the decision as to the best route to send data across networks. The next layer up is the Transport Layer, which provides error and flow control for higher level network applications. This layer also controls reliability, segmentation, and retransmission of failed segments. Transmission Control Protocol (TCP) and User Datagram Protocol (UDP) operate at this level [23, 24]. The remaining upper layers, Session, Presentation, and Application are not relevant for switching and routing operations. All switching and routing can be handled by the lower three or four layers. Therefore most schemes to control switching for hybrid FSO/RF links are handled at these layers.

3.2 Switching Method

It is usually advantageous to implement switching for hybrid FSO/RF systems on as low a network layer as possible. Usually the higher the level one works at, the greater the latency. This is due to the fact that information in each lower layer is wrapped within the layers above it in a process known as encapsulation. At each stage, as a data packet moves through the layers, the packet header relevant to the current layer must be added or read and removed so the next layer can process the data. This process adds processing and overhead time for the data leaving the application to out across the network.

The lowest and fastest level is the Physical Layer. However, switching cannot be done at the Physical Layer alone since by design the Physical Layer only handles transmission on one link at a time. But the Physical Layer is important in getting parameters to help make switching decisions, such as the received signal power.

The next layer up, the Data Link Layer, has some error checking ability but is still unable to perform switching on its own. Although switching at this level is possible with the addition of a specially designed network switch. The switch could be designed to read the frame data, and using the signal power and error information, make decisions on which link to use. However, designing and implementing such a controller is no easy task. Some commercial systems use a simpler system such as a redundant link controller which transmits redundant data on both FSO and RF links. It then checks the frames from each link for errors and if one is found forwards the error free one to the user. The main problem with this system is the mismatch of data rates on both links [14]. Due to this mismatch, not all data on the FSO link can be duplicated and inevitably some data will be lost. Also, some applications may desire minimal use of the RF link, such as when security is a concern. Therefore constantly sending duplicate data on the RF link would not be a viable option.

The next layer is slower than the other two but has the advantage of being relatively easy to design and implement for. Switching at the Network Layer can be done in a variety of ways. It can use some information from the Physical and Data Link Layers such as received signal power or use data from some other source to make switching decisions. This also gives the most flexibility since switching at the Network Layer is mostly handled by software and not hardware as in the lower levels.

Most routers have the ability to check their neighbor links using HELLO packets, which are specialized echo packets between routers, on the Network Layer. However this only provides a rudimentary method of monitoring and switching between links during outages.

One metric commonly used to determine the quality of a link is the bit error rate (BER). The BER is a measure of the total number of bits incorrectly received to the total number sent. It is commonly measured by sending a pseudorandom binary sequence across a link and counting the number of incorrect bits received at the other end. One group designed a system where data between the FSO and RF links were dynamically switched using average measured BERs. They measured the BER every minute and used a sliding average window for measured BER, ranging from 1-100 minute intervals, to determine switching times. They noticed if too short a window is used the link will switch unnecessarily frequently and too long a window allowed longer than acceptable connection outages [7]. However, BER testing is usually done with specialized test equipment and may be impractical in situations where the necessary equipment for testing is unavailable.

3.3 Coding Method

One method of maximizing the use of a hybrid RF/FSO system using specialized coding was proposed by one group. In this system, both the RF and FSO links are utilized to their fullest at all times. They do this using something called non-uniform Low-Density Parity-Check (LDPC) codes [25]. LDPC codes are a type of error correcting code which allows for the transmission of data on a noisy channel at close to the theoretical maximum rate. This is done by encoding data with something

called a parity-check matrix. Encoding the data produces a codeword which is then transmitted across the noisy channel. If any errors occur in the codeword during transit, the decoder at the other end is able to reconstruct the original data.

Theoretically the maximum possible data rate for a given amount of noise can be matched arbitrarily close by using appropriate code word lengths [26].

Non-uniform codes are designed to code data over a set of parallel sub-channels. The non-uniform LDPC code the group developed has better performance than regular LDPC codes since non-uniform codes are optimized using channel information. It is also better able to handle bursty channels, which is the nature of FSO channels. The code was designed to handle encoding and decoding for all the channels which provides diversity, compared to using separate encoders and decoders for each separate channel in regular LDPC codes. However, regular coding schemes are designed for time-invariant channels, which is not the case for FSO. The group decided to introduce a way to adjust the rate the error correcting code works at, depending on channel conditions. They do this by varying the length of the codeword used. When the channel is working well the codewords can be made shorter to increase the effective data rate. When the channel experiences drops, the codeword can be made longer to improve error correction [25].

Although the details of how to measure the capacity of a channel at any given time is yet to be addressed, this system looks promising for maximizing the use of the available capacity of a hybrid RF/FSO system. The use of an error correcting scheme inherently allows for an arbitrarily low BER, but this comes at a tradeoff of added complexity and latency due to the encoding and decoding process.

Of all the various techniques for monitoring and utilization of hybrid RF/FSO systems, each has its own advantages and disadvantages. Some are better suited for certain situations than others and therefore tradeoffs need to be made in terms of practicality and effectiveness.

Chapter 4: Experimental Setup

The quality of any communication link is determined by the amount of data that can be sent across it reliably. This is related to the ratio of the number of packets received to the number of packets sent. Using this metric, the general quality of the FSO link can be determined in order to selectively route information between it or an RF link. One of the issues that need to be addressed when combining RF and FSO links is determining optimized path selection to route the information quickly and robustly. The quality of the FSO link can be determined in part by detecting the scintillation present across the link. Since scintillation is always present in an FSO link and is usually the most important factor outside of total loss weather events such as fog or rain. In most applications, a scintillometer is not available to provide this information. A simpler and more universally applicable method is desired. Therefore a software based switching system using echo packets was used. Echo packets can be used on any system that can use TCP and Internet Protocol (IP), regardless of the underlying hardware.

For testing, attenuation from scintillation was chosen to be simulated since the most interesting results can be seen from this kind of atmospheric effect. The quick and intermittent dropouts it can cause will be able to test the system's switching ability more rigorously than more steady and longer term effects like fog.

4.1 Setup

To characterize the FSO/RF links under controlled conditions, two paths were configured, as shown in Figure 4-1.

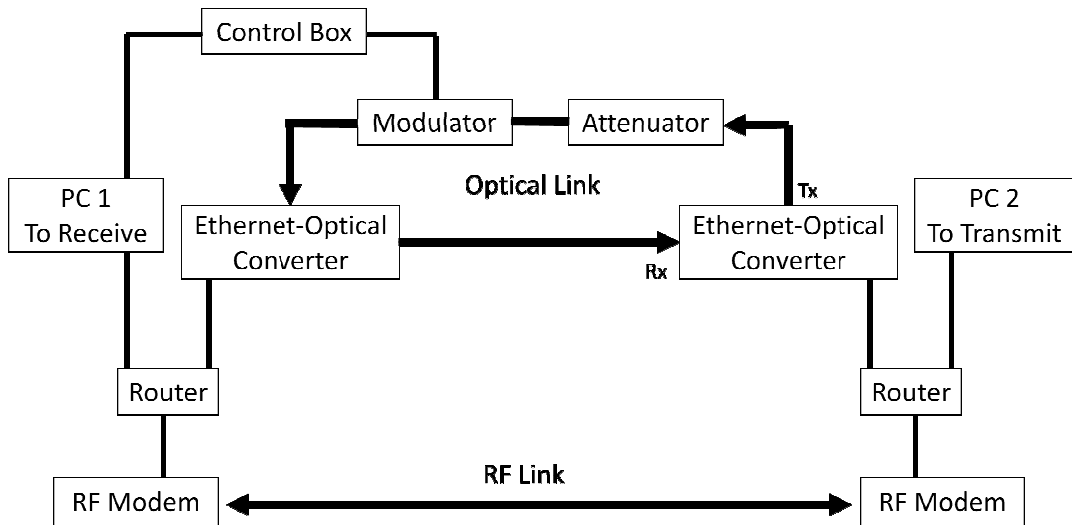


Figure 4-1. RF/Optic link configuration.

The RF link was setup between two Comtech SDM-300 Satellite Modems set to transmit at 2 Mbps through coaxial cable. A cabled link was chosen to eliminate any possible external interference and to maintain a consistent link. The routers used were the Cisco 1841 Integrated Services Routers with serial and Ethernet interfaces for the RF modems and PCs connections respectively. The modems and routers are shown in Figure 4-2.



Figure 4-2. RF modem and routers

The Cisco routers were configured to use the Enhanced Interior Gateway Routing Protocol (EIGRP) for routing data between the optical and RF links. EIGRP is a Cisco proprietary distance-vector based routing protocol. Like all routing protocols, EIGRP maintains a routing table of known paths to different network destinations. It then uses a number of metrics to determine the best available path to send packets. If the status of any of the paths in the routing table changes, the routers sends the changes to its neighbor routers to update their routing tables as well. By default, the optical path is set to be chosen with the RF path as backup. In order to switch data transmission at a desired point in time, the routing table can be modified in one of the routers to make it use the RF path. This change will then be sent to the other router automatically causing it to change paths as well. The routing tables were configured according to the network map shown in Figure 4-3.

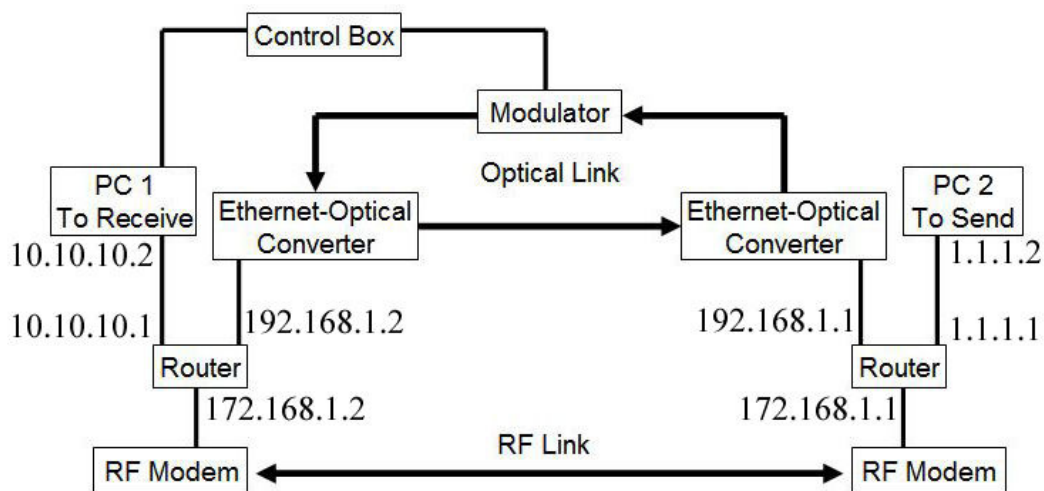


Figure 4-3. Network map.

The monitoring and switch handling was all done on just one side of the link (PC 2) instead of both sides. This simplified the setup and doesn't require continual synchronization of both ends for switching. Since echo packets and their responses

travel across both directions of the link, pinging from one side is usually all that is necessary in order to see a working full duplex link.

An FSO link was simulated using fiber optics. This allowed the optical part of the link to be tested and simulated in a controlled and reproducible environment. The attenuation effects of the atmosphere were emulated using an adjustable attenuator and an optical modulator. The attenuator type was a graded neutral density filter where the level of attenuation can be adjusted by turning a screw on the side as shown in Figure 4-4. The attenuator was used to apply a constant level of attenuation when needed.

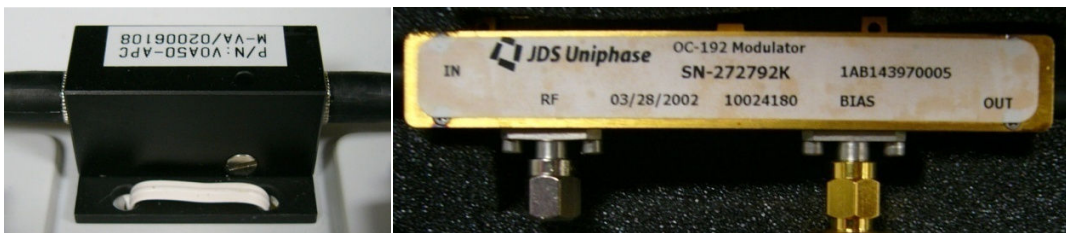


Figure 4-4. Attenuator (left) and modulator (right).

Also shown in Figure 4-4, is the optical modulator. The modulator is the most important part of the setup since it is used to simulate attenuation effects from scintillation. The modulator was controlled using a National Instruments Shielded Connector Block BNC-2110 connected by a National Instruments DAQCard-6036E to a laptop PC. The whole modulator system was controlled by Labview on PC 1.

The actual data transmission and network performance measurements were handled by a program called the Multi-Generator (MGEN), developed by the Protocol Engineering Advanced Networking Research Group at the Naval Research Lab (NRL) [27]. MGEN is capable of generating network traffic patterns by sending data across a network over time and measuring the data rates and packets dropped along

the way. For this project, it was configured to send packets using User Datagram Protocol (UDP) at a rate of 20 Mbps, with packet sizes of 1472 bytes. Compared to Transmission Control Protocol (TCP), UDP sends packets with no guarantee of delivery so it does not try to resend packets that are lost. This allows for constant transmission at a set speed even with losses and therefore the raw carrying capacity and full losses of a link can be seen. Whereas TCP calls for the speed of transmission to be dropped whenever there is a loss of packets.

For all tests, data from MGEN is transmitted in only one direction, from PC 2 to PC 1. Due to the fact that only one modulator was available to use.

4.1.1 Modulator

The modulator type used in this setup is a Lithium Niobate (LN, LiNbO_3) Mach-Zehnder (MZ) modulator. This type of modulator is commonly used in the telecommunications industry. The LN crystals used in MZ modulators use the electro-optic effect, in particular the Pockels effect, to modulate light. The electro-optic effect describes how the index of refraction in a material can change with an applied electric field [28].

A typical MZ modulator has a layout as shown in Figure 4-5. A waveguide path of LN is split into two equal length arms. Two pairs of electrodes are applied to the wave guide. One for a direct DC bias and another for high frequency signals.

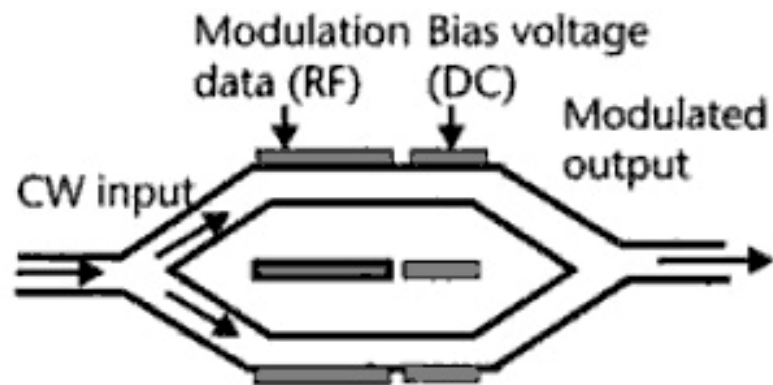


Figure 4-5. Mach-Zehnder modulator layout.

In coming light is evenly split along the two arms. When a voltage is applied the index of refraction of the LN arms changes due to the electro-optic effect. When the index of refraction increases as a result, the speed of the light travelling through slows down. This effectively retards the phase of the optical signal. When the index of refraction is the same in both arms, the light from the two paths will arrive at the other end at the same time and combine constructively. However, if there is a difference in the index of refraction between the two arms, the light from each side arrive at the end with different phases and destructively interfere with each other. This will lower the light power output at the other end, and in the extreme case where the phase difference is 180° the two beams will completely cancel each other and no light will come out. The voltage where this condition occurs is called V_π and is dependent on the modulator's layout design. Usually the electrodes are placed in a way such that an applied voltage will create opposing changes in the index of refraction in both arms. An equation describing how the inputted optical power is affected is shown in Equation 4.1.

$$P_{\text{out}} = P_{\text{in}} \cos^2\left(\frac{\pi V}{2V_{\pi}}\right) \quad (4.1)$$

Here P_{in} and P_{out} are the power going in and coming of the modulator respectively. V is the total voltage applied from both the DC bias and high frequency modulated inputs [29]. Shown below is a fitted curve of the transmission vs. voltage for the modulator used in tests.

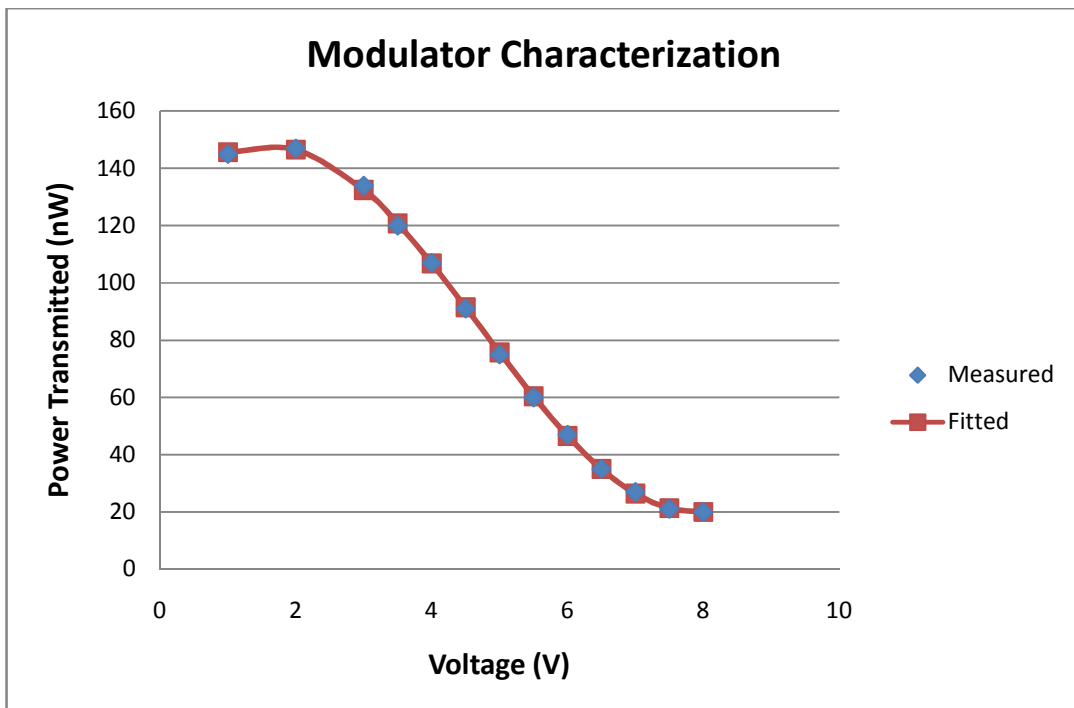


Figure 4-6. Transmission curve for modulator.

This characterization curve was obtained by applying a constant voltage to the modulator and measuring the output power of light for different voltages. The points were then fitted using Equation 4.1. The initial input power was lowered with the attenuator in order to bring the range of the curve around the operating threshold of the optical media converters. V_{π} was found to be about 7.9 volts, and in practice the mutual cancellation at V_{π} is not perfect so there is still some leakage of light out the

other end as one can see in Figure 4-6. Also the peak of transmission is not at 0 volts but at around 1.6. This may be due to the fact the path lengths of the two arms are not exactly the same so there will be some slight cancellation even at 0 volts. Adding some voltage can bring the two paths back in phase, therefore the peak is shifted from 0.

4.1.2 Media Converters

In order to convert electrical signals to optical for simulation, two IMC MiniMc media converters were used as shown in Figure 4-7.



Figure 4-7. MiniMc Media Converters

These interfaced by Ethernet with the routers and converted the electrical signals into optical and sent through optical fibers. Each MiniMc handles transmit and receive functions and operates at 1550 nm wavelength. They are connected by single mode optical fibers. In order to characterize their minimum thresholds for operation, power measurements for the transmitted optical carrier and their performance must be made. Power measurements were made using a Newport Multi-Function Optical Meter Model 2835-C. The initial average transmit power was measured to be 0.8 mW.

Using the attenuator, a constant level of attenuation was set and the data throughput performance was measured using MGEN for a period of 60 seconds. Even when attenuated down to 130 nW of average power transmitted, there is virtually no loss as shown in Figure 4-8.

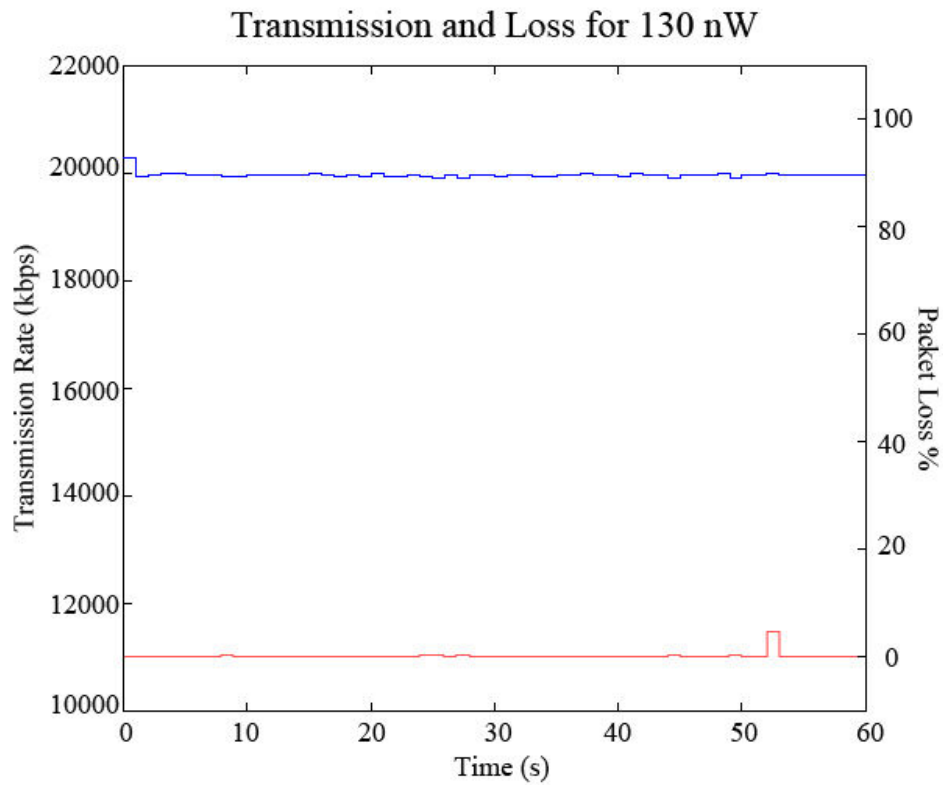


Figure 4-8. Transmission rate and loss of packets for attenuation down to 130 nW. Blue line is the transmission speed and red line is the packet loss.

Attenuation effects only start to emerge when the average power is attenuated down to 120 nW as shown below.

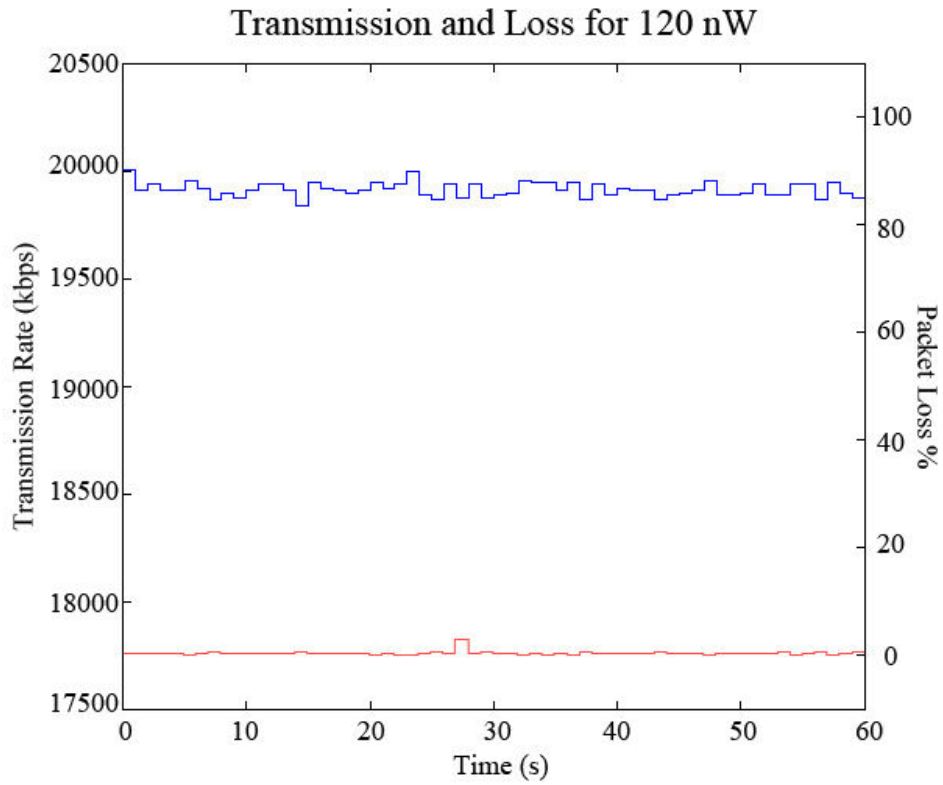


Figure 4-9. Attenuation down to 120 nW.

At 120 nW of average power there is a slight fluctuation in transmission speed just under 20 Mbps and the losses are at a barely noticeable level. As the power is further attenuated the losses steadily increase. At 110 nW of average power, noticeable losses start to occur as in Figure 4-10.

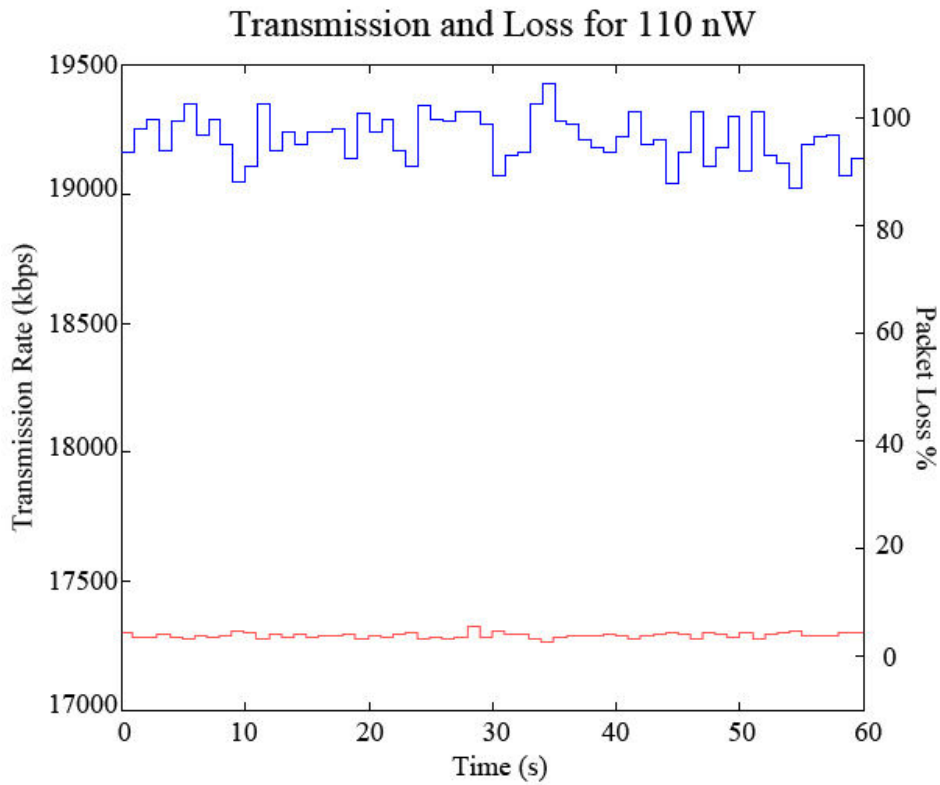


Figure 4-10. Attenuation down to 110 nW.

The average packet losses are now at around 5% and the transmission speed has lowered by almost 10 Mbps. As power is further attenuated the losses steadily increase. Transmission and losses for attenuation down to 100, 90, and 80 nW can be seen in Appendix A. The optical link is barely maintained down to 70 nW of attenuated average power. As seen in Figure 4-11, the packets losses are nearly 100% and the transmission speed is down below 2 Mbps.

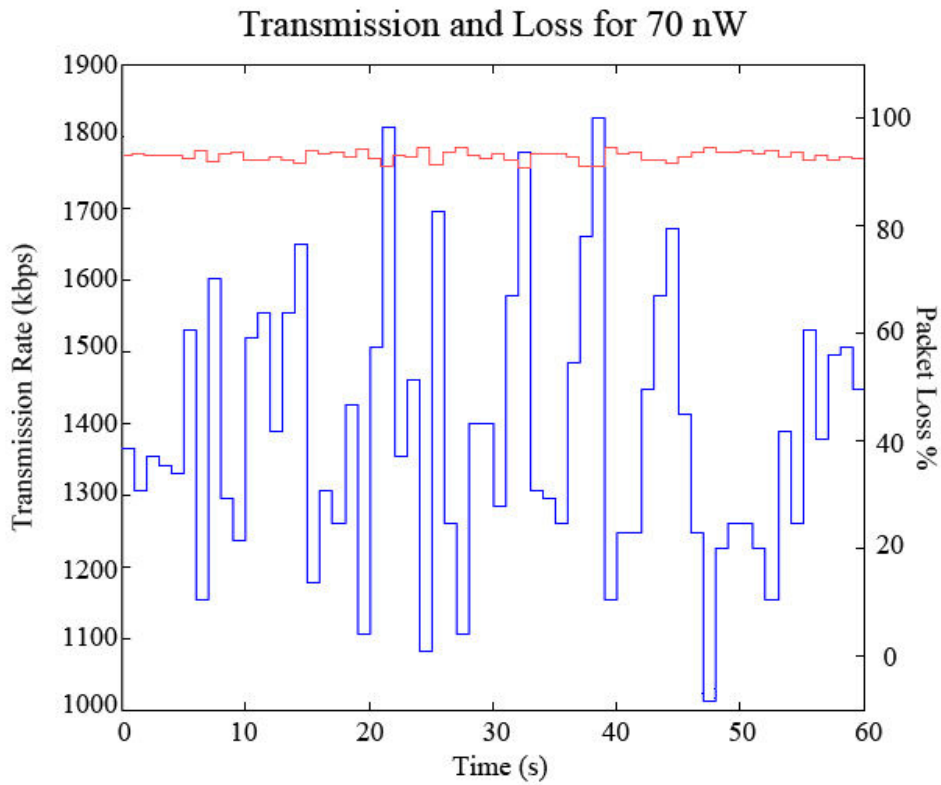


Figure 4-11. Attenuation down to 70 nW.

Any further attenuation below this point causes a total loss in the optical link. Based on these measurements, the point of 110 nW and 70 nW were picked as the transition boundaries for optical link loss. Starting at 110 nW where the link starts to gain noticeable losses down to 70 nW where there is total link loss below that level.

4.2 Scintillation Data and Switching Program

For the modulator to simulate atmospheric attenuation from scintillation and other sources, an appropriate signal must be inputted. For this purpose, scintillation data taken from the NRL Chesapeake Bay detachment was used. The data is a real time measurement of the optical power received across a distance of 500 m on a clear day. This data was then read and converted into a format that could be used as a

signal for the modulator. A Matlab script processed the data and it was scaled using the modulator's characterized transmission curve from Figure 4-6. It was sampled at 100 Hz and a 100 second span was taken to be used in tests, as seen in Figure 4-12.

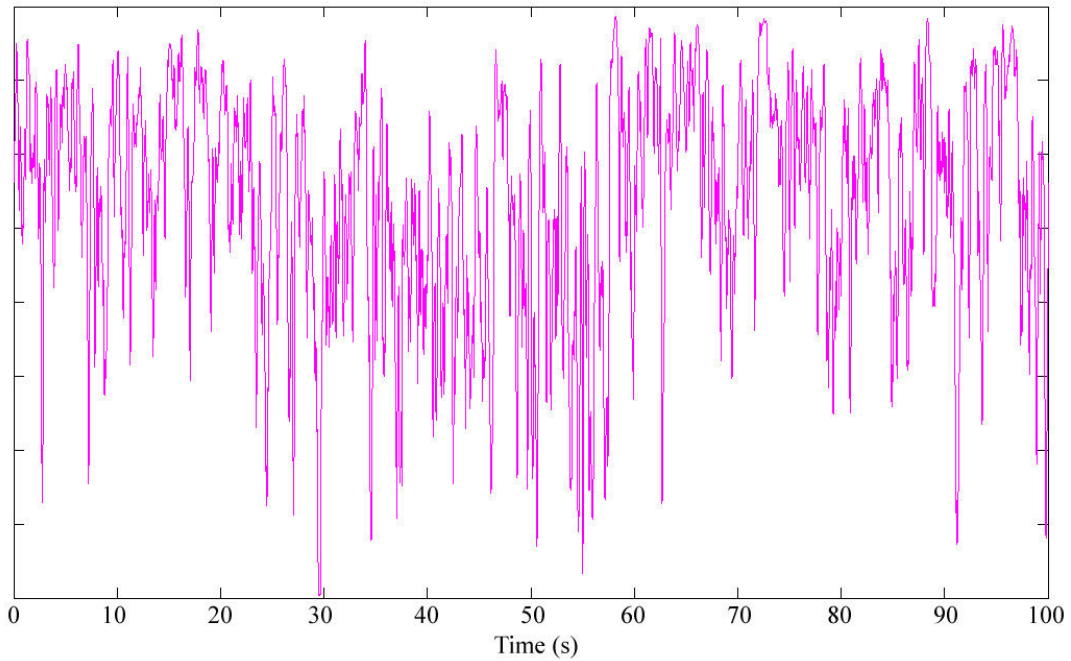


Figure 4-12. Formatted scintillation data.

The same set of data was used for all tests except for the scaling of the signal. The effect of scintillation was either magnified or reduced to test for different level conditions. The most interesting tests for switching would be for scintillation occurring around and across the threshold for maintaining optical link. Therefore the data was scaled to cross this threshold by different amounts for testing.

The actual switching was performed using a C++ program written to send echo packets, also known as pings, across the optical link to determine link quality. Echo packets work on the Network Layer and use the Internet Control Message Protocol (ICMP). These packets are typically used to check if a certain host or

destination on a network is reachable. If they are successfully received at the destination, a response is sent back acknowledging the sender. Therefore both the transmission and receive channels on a link must work in order to receive a successful response for an echo packet [23]. The program used for switching was set to send echo packets every 100 ms across the optical link. Over a set period of time the program would keep track of how many echo packets were successful and how many were lost. It would keep a running average and tell the router to either switch data transmission from the optical link to the RF link or vice versa. This is done by the program modifying the routing table in one of the routers forcing it to send data on the desired link path. These switching decisions are based on three main parameters defined by the user for the program. The first is the size of the averaging window for the number of echo packets dropped. The second and third are what percent of packets dropped is needed to switch from optical to RF and what percent is needed to switch back. These parameters can be adjusted to cause the system to be more or less sensitive to link outages by adjusting the packet loss level and averaging window sizes.

Chapter 5: Data and Results

5.1 Initial Performance Measurements

5.1.1 MGEN Data

In order to find the optimal parameters and to test the switching program, transmission speed and loss packet data was taken using MGEN. The scintillation data was scaled to cause anything between slight to severe optical link quality loss. First, an initial run of five runs were made using only MGEN to see the effect the simulated scintillation would have on transmission speed and packet loss.

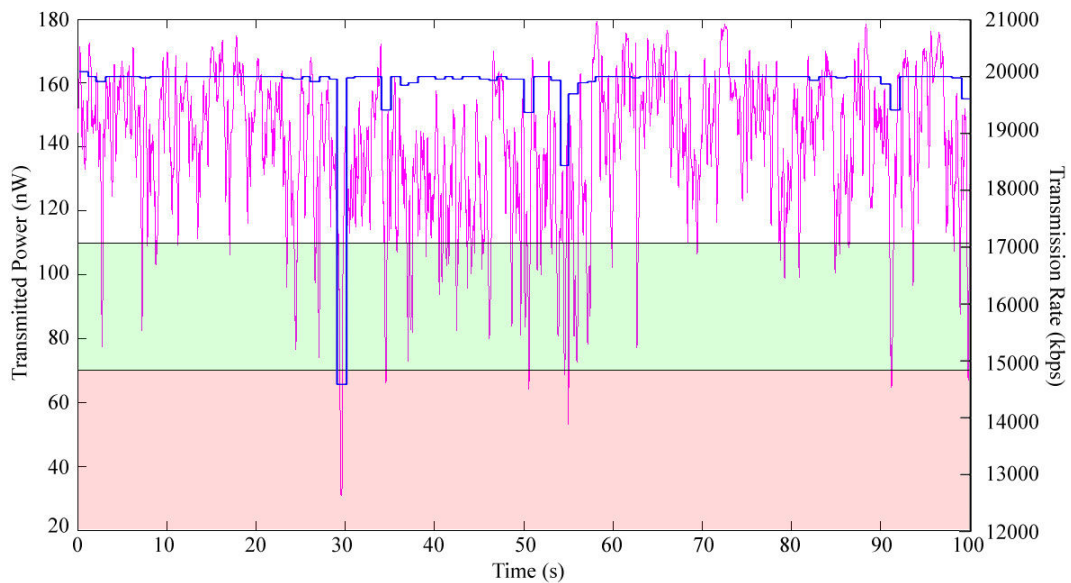


Figure 5-1. Transmission rate for minimal degradation of link quality. The transmission rate is in blue and scintillation data is in magenta. The green area represents the threshold for optical link loss, ranging from 110-70 nW. Any power that falls below 70 nW into the red area represents total loss of optical link.

In Figure 5-1, one can see that when scintillation is barely starting to cross the threshold for transmission, found in 4.1.2, the transmission rate still holds fairly

steady at its initial set speed of 20 Mbps. The speed only drops noticeably when the scintillation starts to dip into the red area. This is especially noticeable for one spike at 30 seconds where there is a corresponding sudden drop in transmission speed. The corresponding packet loss data for Figure 5-1 is shown below.

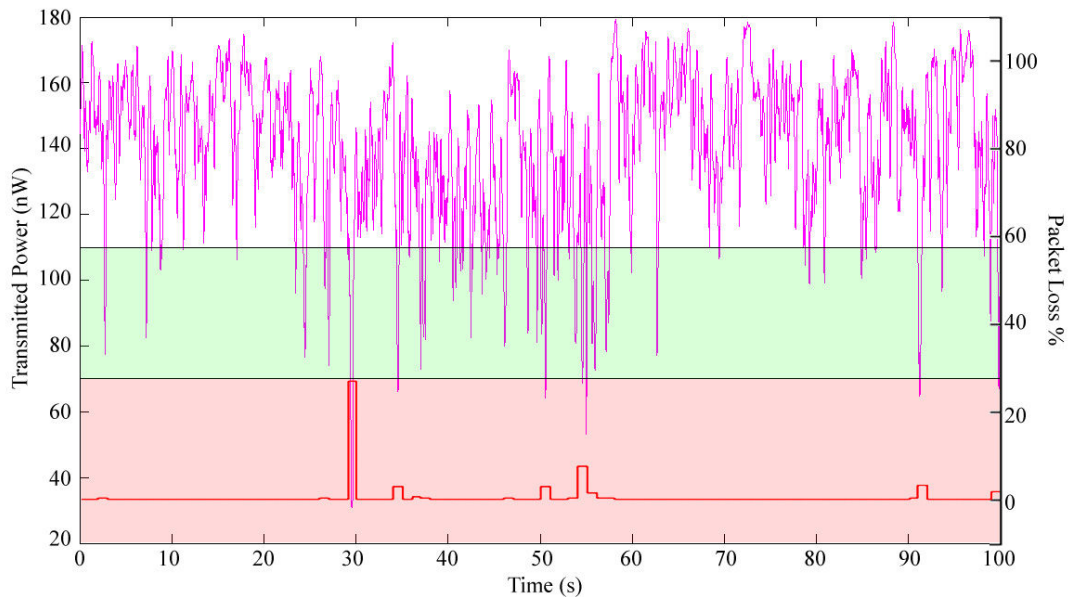


Figure 5-2. Corresponding packet loss data for Figure 5-1. The packet loss is in red and scintillation data still in magenta.

Here as one would expect, with a drop in transmission speed in Figure 5-1, there is a corresponding effect in packet losses, with the same spike in loss seen at 30 seconds.

Transmission and packet losses were measured again with the scintillation scaled for a deeper fade (wider range of attenuation) as shown in Figures 5-3 and 5-4.

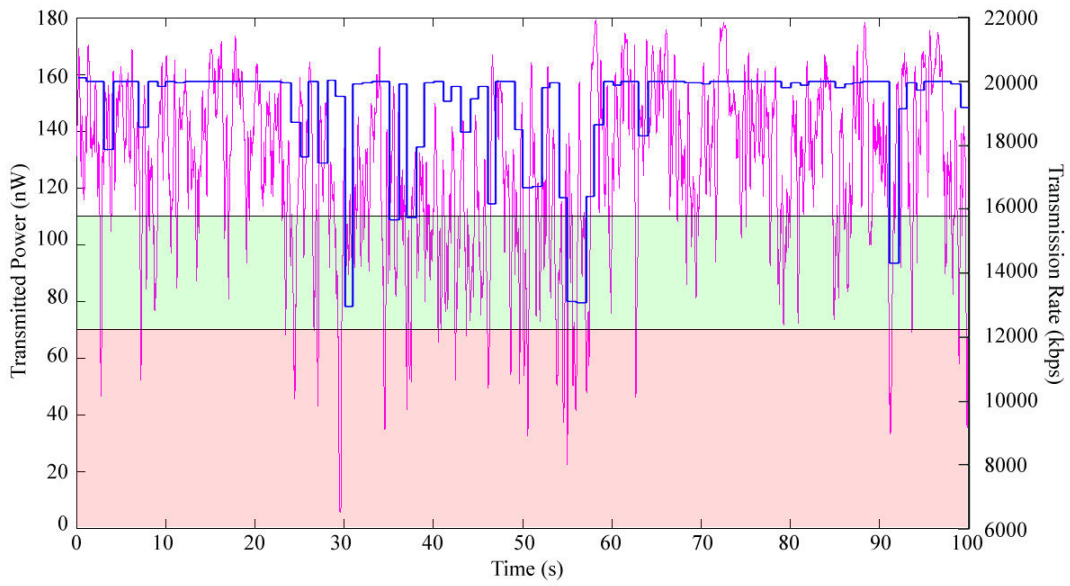


Figure 5-3. Transmission rate for increased fade.

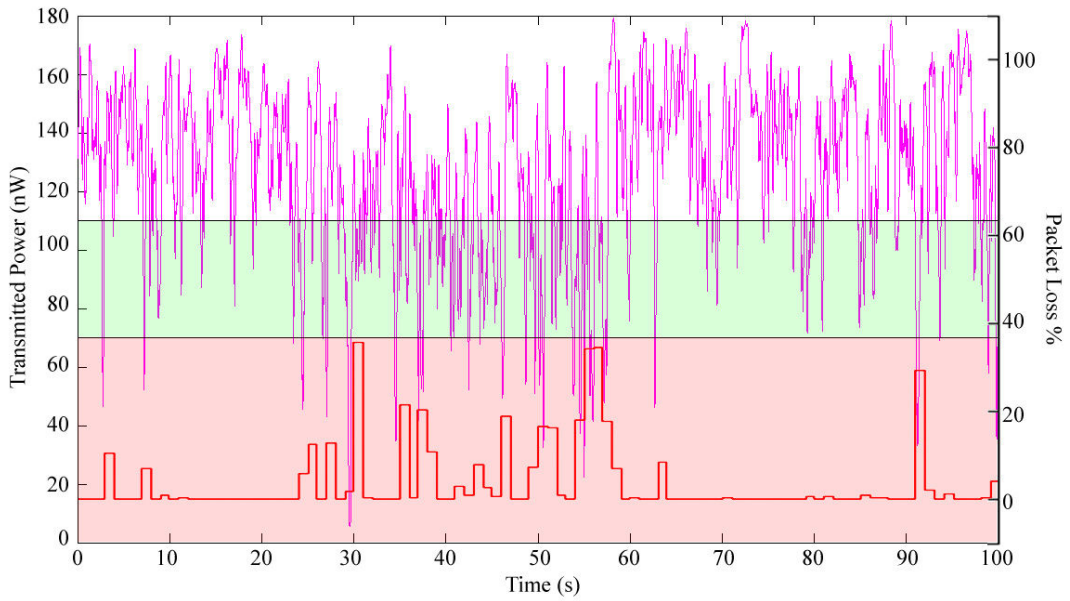


Figure 5-4. Packet loss for increased fade.

Here more of the scintillation crosses the threshold level into the red area. There is noticeable loss in transmission speed and packet loss. All the drops in speed are mirrored as packets lost due to the fact that UDP does not resend data and there is no

guarantee of delivery. At this level, the loss of optical link quality is still moderate and not too serious with only a few drops. The graphs below show transmission and packet losses for the deepest amount of fade tested, Figures 5-5 and 5-6.

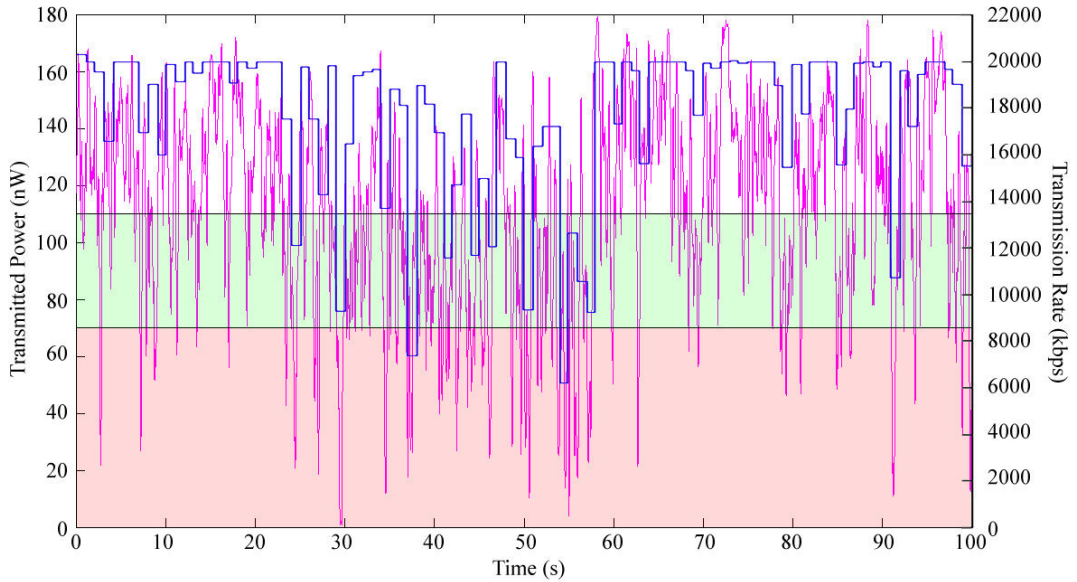


Figure 5-5. Transmission rate for maximum fade.

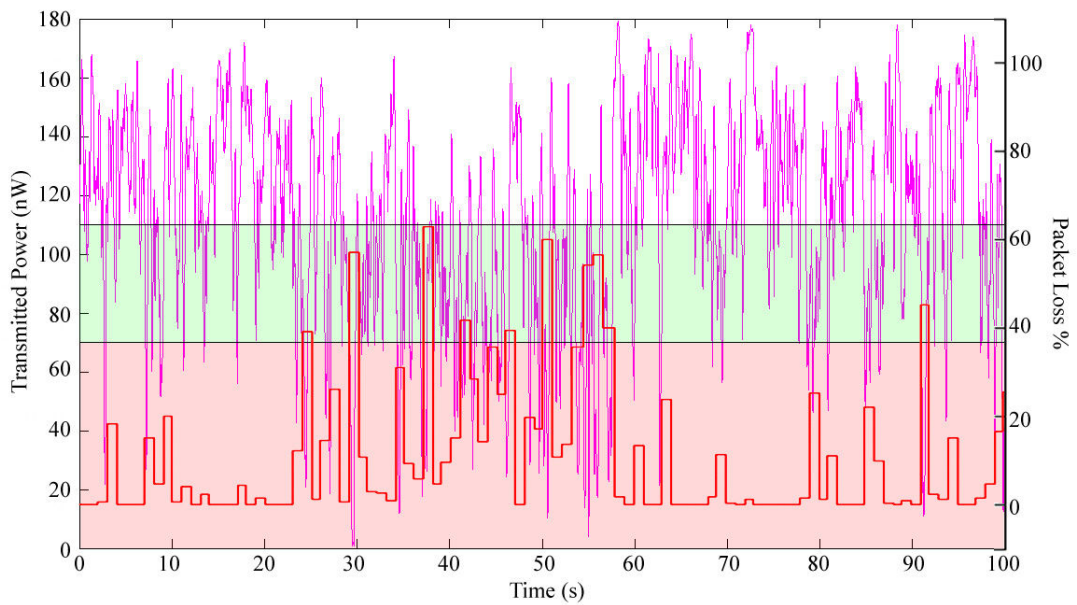


Figure 5-6. Packet loss for maximum fade.

Here one can see there is a significant loss of packets and drop in transmission speed. For a span of about 30 seconds, packet losses were about 30% or more with peaks near 60% at some points. Such losses may warrant switching to the RF backup link for a period of time even though the speed is not greatly diminished; too many lost packets affect data quality and in the case of TCP cause a lot of extra traffic overhead since packets need to be resent if lost. In the next two figures, the fade was lessened but the overall effect of scintillation was increased, lowering the average transmitted power. This brought more of the scintillation in and below the threshold level.

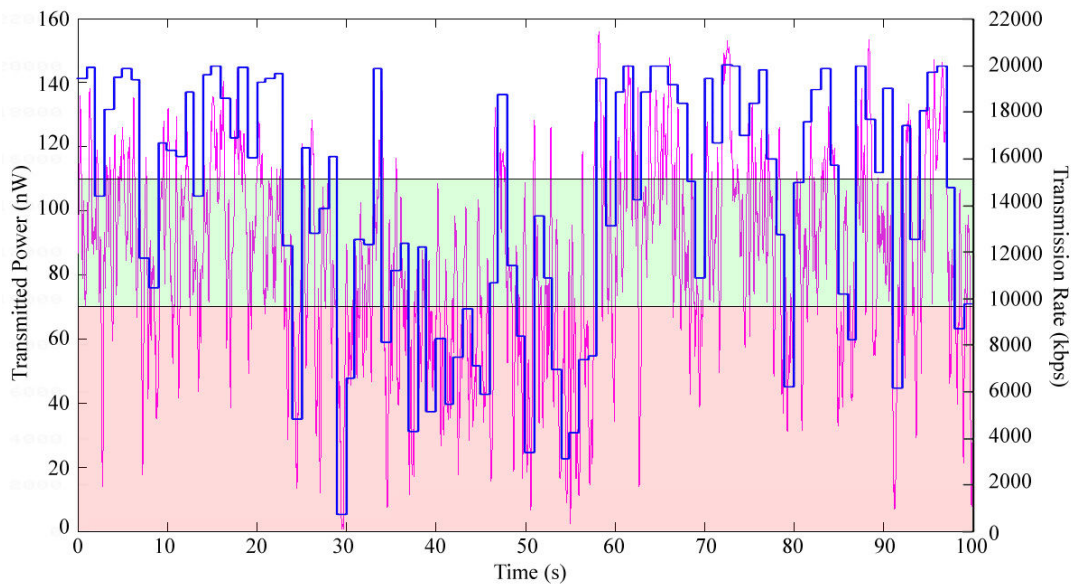


Figure 5-7. Transmission rate for greater scintillation (greater attenuation).

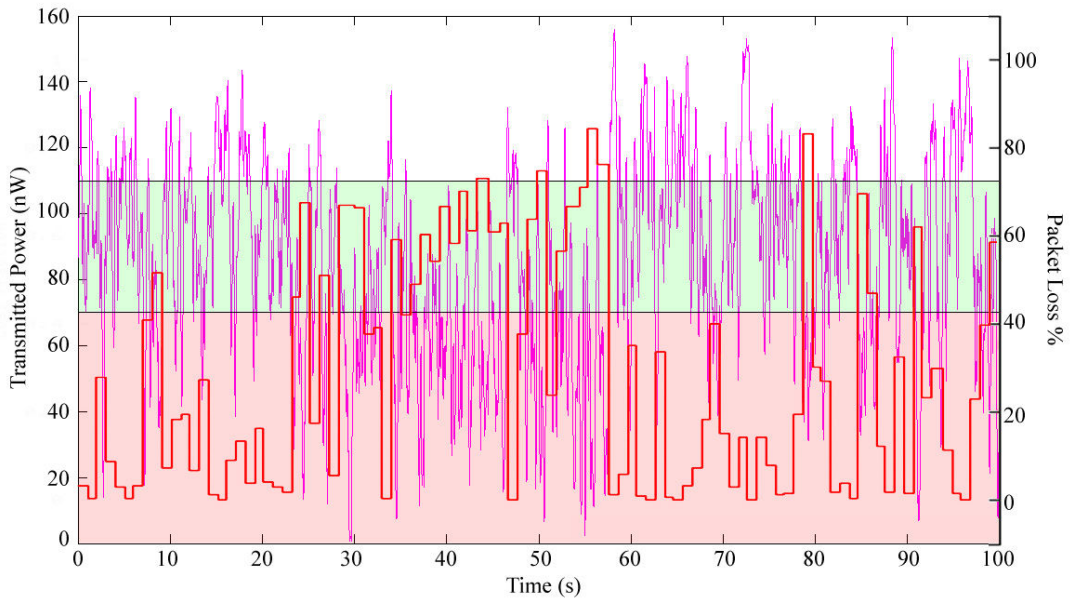


Figure 5-8. Packet loss for greater scintillation.

In this run the speed is greatly reduced, dropping to 4-2 Mbps at some points. Losses are also peaking around 80% with an overall loss of at least 30% or more for a significant portion of time. In the last run, the attenuation from scintillation was further increased where almost all the scintillation was crossing or below the threshold level.

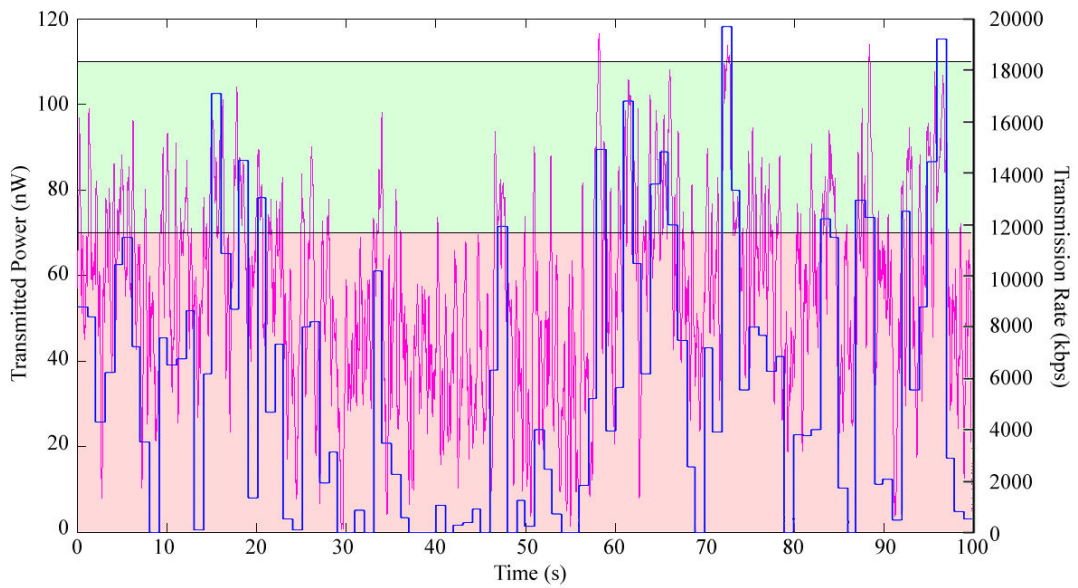


Figure 5-9. Transmission rate for greatest level of scintillation.

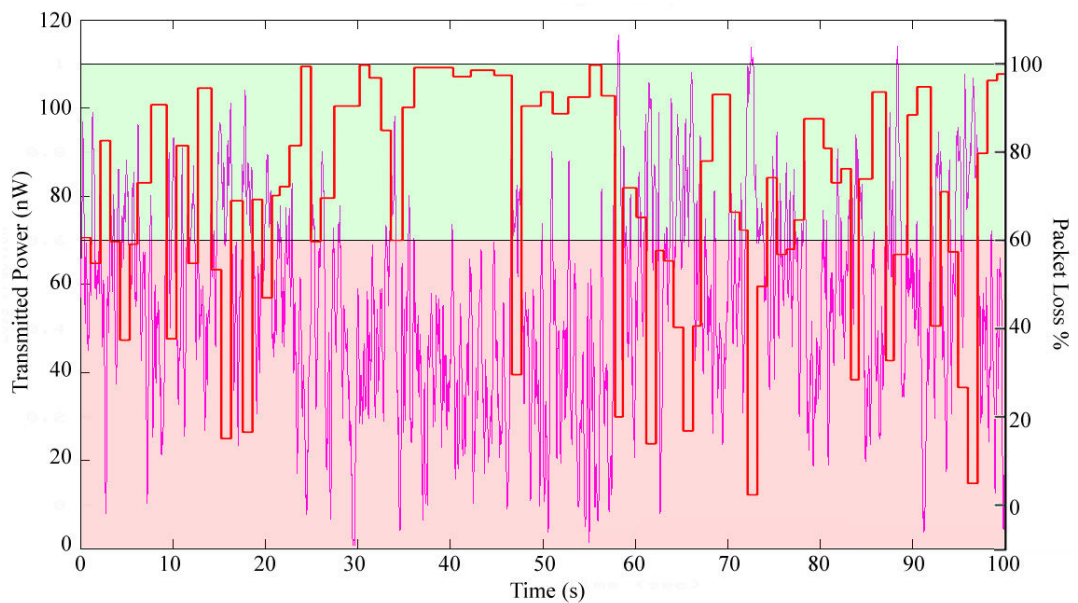


Figure 5-10. Packet loss for greatest level of scintillation.

Figures 5-9 and 5-10 show the transmission speed range is very wide and erratic. For the majority of the time the speed is below half the original set speed and at certain times the speed actually goes to 0. The packet losses reflect this, showing greater

than 50% losses most of the time with some points at 100% loss. At this point it is reasonable to say that the optical link is unusable or highly unreliable at best. Any increase in scintillation will most likely cause a complete loss of connection since even at this level packets must be forcibly pushed through with a great deal of loss. Ideally a switching algorithm or program will switch to the backup RF link before too many losses accumulate from a degraded link condition such as in the case above.

5.1.2 Echo Packet Losses

Next, the effects of scintillation on echo packets sent by the switching program were studied. The scintillation scale with the deepest fade was chosen to run echo packet loss tests, since this gave conditions of both acceptable and unacceptable optical link quality within a single run. The tests were done for various averaging window lengths. Windows from 5-100 seconds were chosen and the losses measured. All the runs are overlaid as red lines in Figure 5-11 below.

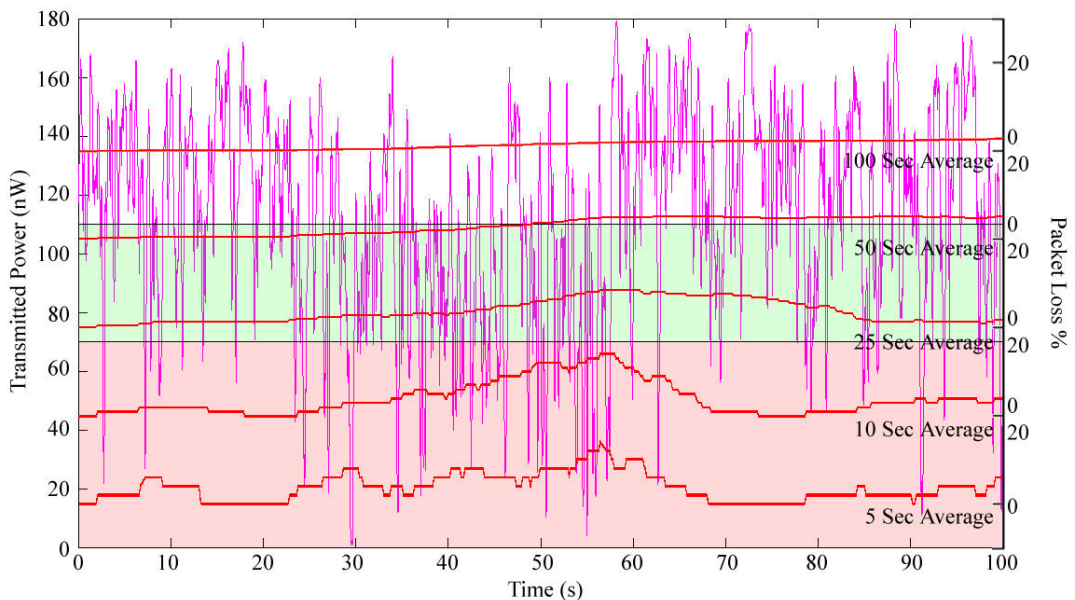


Figure 5-11. Echo packet losses for 5-100 second averaging intervals.

For each of the runs, the loss rate never exceeded 20%. In contrast loss rates in Figure 5-6 peaked around 60% a few times. This is mainly due to the fact that the echo packets were only being sent every 100 ms while data transmitted at 20 Mbps send over 1500 packets a second depending on packet size. The greater the number of packets sent the greater the chance for a drop. As one would expect, the longer the average window the more smoothed out the losses become. The 5 second average peaks at 14% echo packet loss with a total of 26 packets dropped over the whole run. The 100 second average run only reached 2.8% loss with a total of 28 packets dropped the whole run. Although the total number of echo packets dropped was similar in each run, the shorter averaging window is able to “see” more of the scintillation. Overall, most of the runs showed a 5% or greater loss during the time where scintillation was strongest. Therefore 5% loss or greater was picked as the parameter for switching to RF for the next stage of testing. For switching back to the optical link, 2% loss or less was picked as the parameter, since for the five second averaging window size, this equates to one packet loss within every five second window.

Of course since the scintillation is only affecting the transmit side of the fiber optics and not the receive side, the actual echo packet success rate would be lower in a real world setting, when subject to the same kind of scintillation. Since all echo packets need to have an acknowledgement sent back through the same atmosphere there is a higher chance that even if the echo packet made it to its destination, the acknowledgement packet may get lost on the way back. Even with just one side being affected in the simulated tests, the results are still valid for determining and

measuring switching parameters and characteristics. In this case, data is only being sent in one direction so checking one side is enough for testing. In the case where data is being sent in both directions, echo packets can automatically check both channels since a round trip is needed for success.

5.2 Switching Performance

5.2.1 Scintillation Affected Switching

In the next set of runs, the switching program was fully enabled with the parameters determined in 5.1.2. MGEN was run again with the switching program using the same deep fade level of scintillation as in the previous section. Switching to RF was set at 5% echo packet loss or more and switching back to optical was set as 2% loss or less. The first run was made for a 50 second averaging window and is shown below.

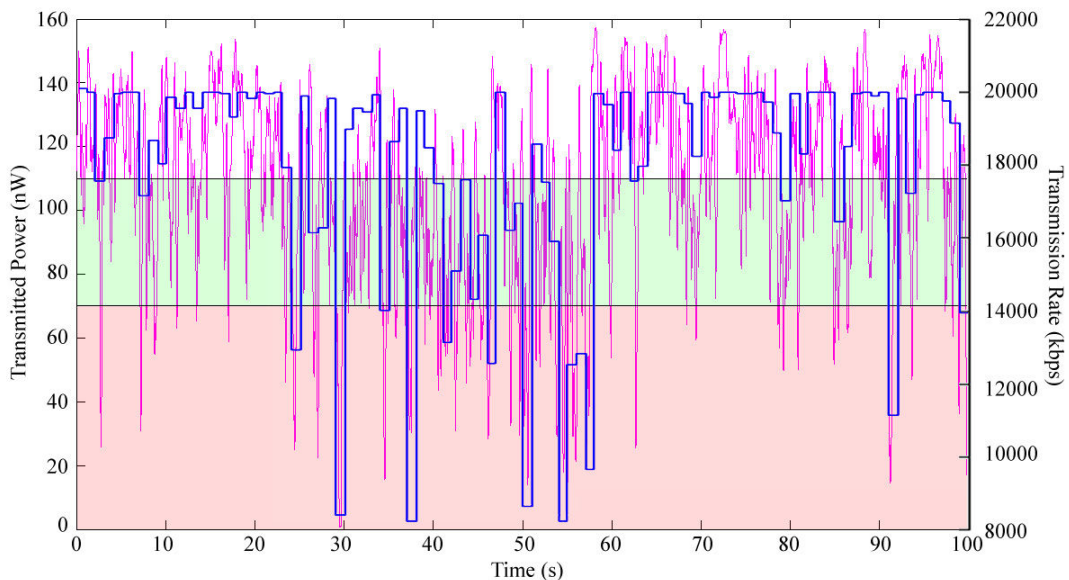


Figure 5-12. Transmission rate for 50 second averaging window.

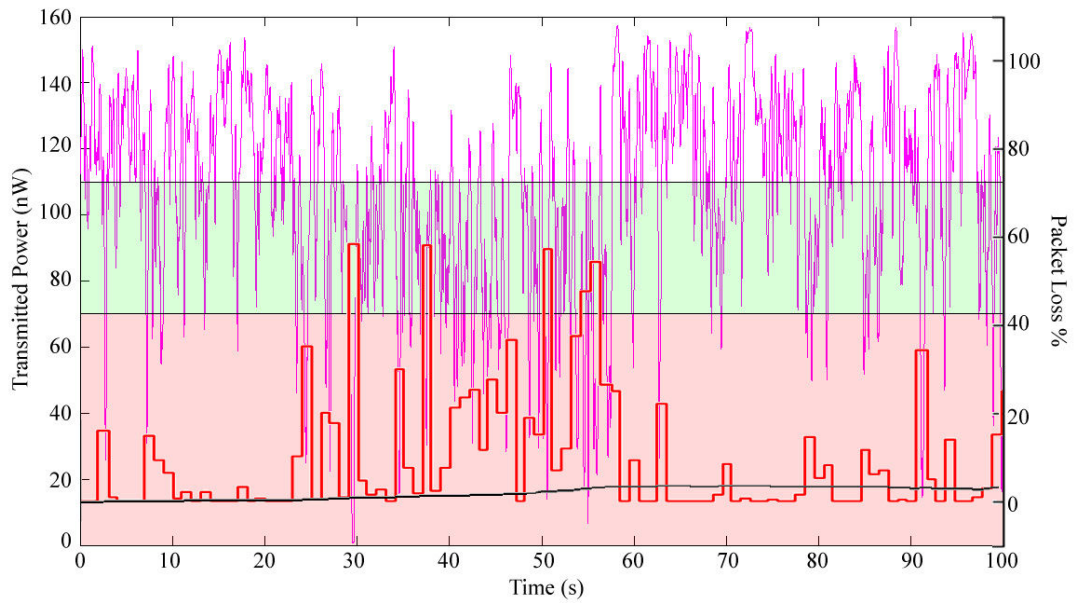


Figure 5-13. Packet loss for 50 second averaging window. The red line represents MGEN packet losses and the black line represents echo packet losses, with magenta continuing to represent scintillation.

For the 50 second run, the averaging window was too long to trigger switching. The loss peaked at 3.6% with a total of 23 packets dropped over the whole run. In this case, the switching program was insensitive to the level and duration of scintillation used. The next run was made with a 25 second averaging window as shown below.

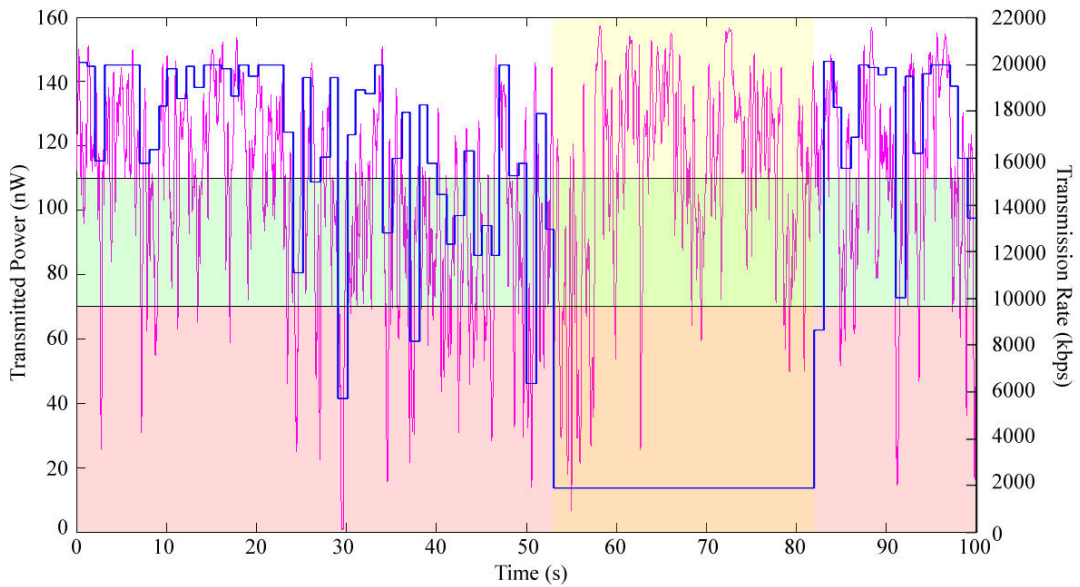


Figure 5-14. Transmission rate for 25 second averaging window. The yellow area represents when the router is switched to the RF link and is active.

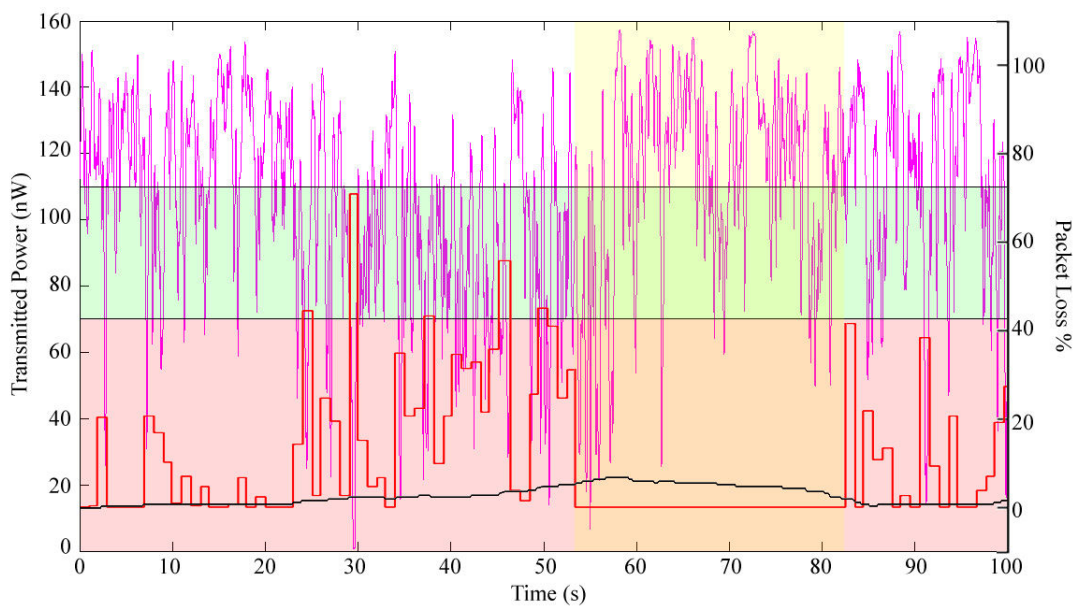


Figure 5-15. Packet loss for 25 second averaging window.

Compared to the 50 second run, the 25 second run reached a high enough loss percentage to trigger a switching event. This is represented by a yellow area starting around the 53 second mark and lasting until around the 82 second mark, for a total of

about 29 seconds of RF use. The echo packet loss peaked at 6.8% with 23 packets lost total and crossed the switching threshold of 5% at 53 seconds. The threshold for switching back to optical was crossed at 82 seconds. Figure 5-14 shows how the transmission rate is dropped to 2 Mbps when sending on the RF link. Although the speed is much lower than when using the optical link, the connection is much more reliable with none of the large packet dropouts one would experience if still on the optical. The next run was made using a 10 second window.

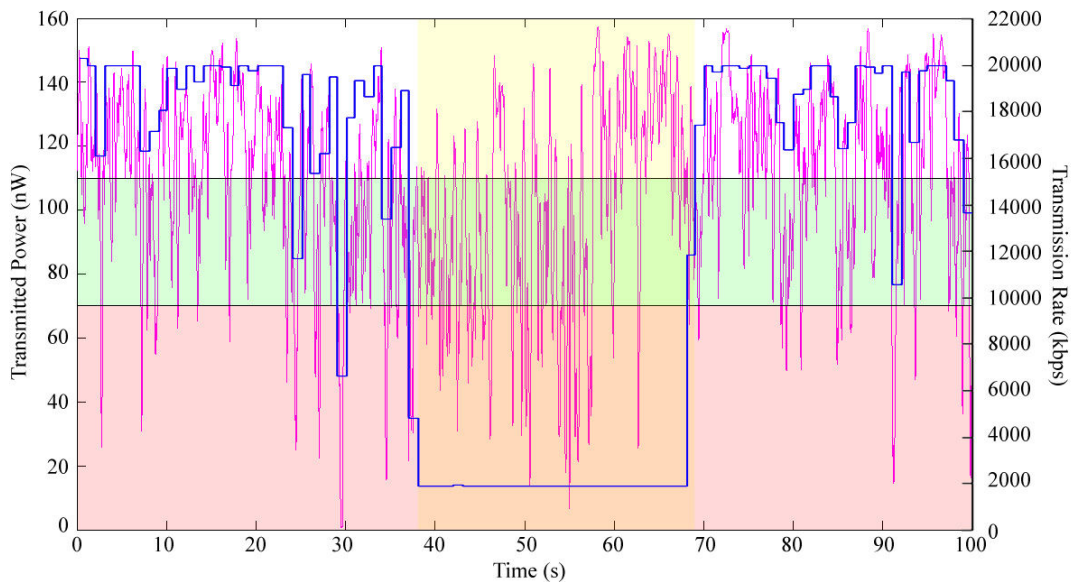


Figure 5-16. Transmission rate for 10 second averaging window.

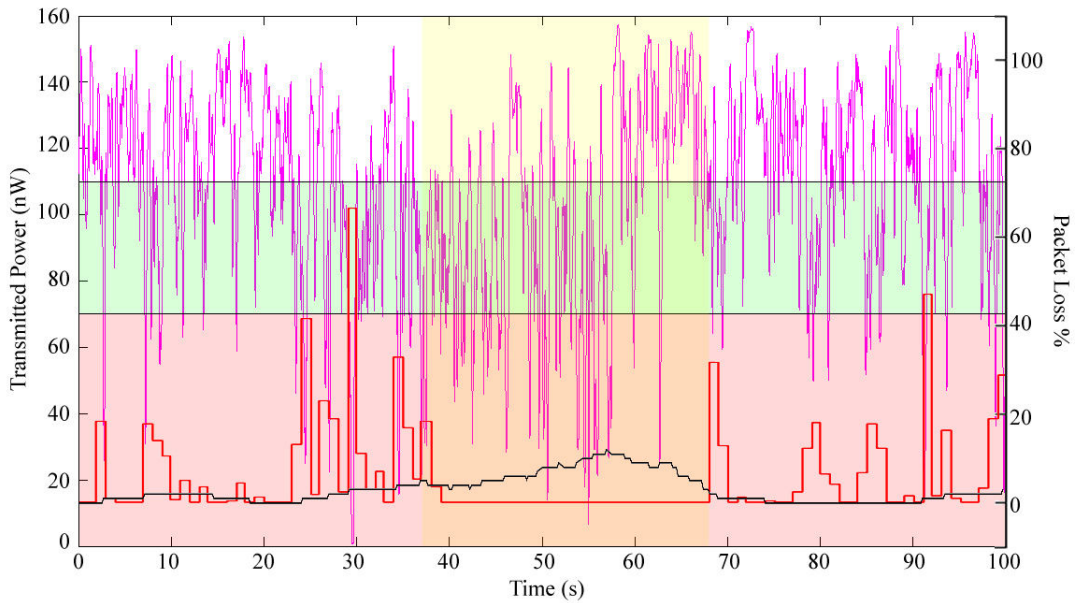


Figure 5-17. Packet loss for 10 second averaging window.

The 10 second run looks similar to the 25 second run. The main difference is that in the 10 second run the system was switched to the RF link earlier, starting from around 38 seconds until about 69 seconds. RF use lasted about 31 seconds with a loss peak of 11% and total packet loss of 23 packets. Compared to the 25 second run, the 10 second run provided a quicker response to the drop in optical link quality by switching to the RF link 15 seconds earlier and then switching back more quickly as quality improved. Last, a 5 second averaging window run was made as shown below.

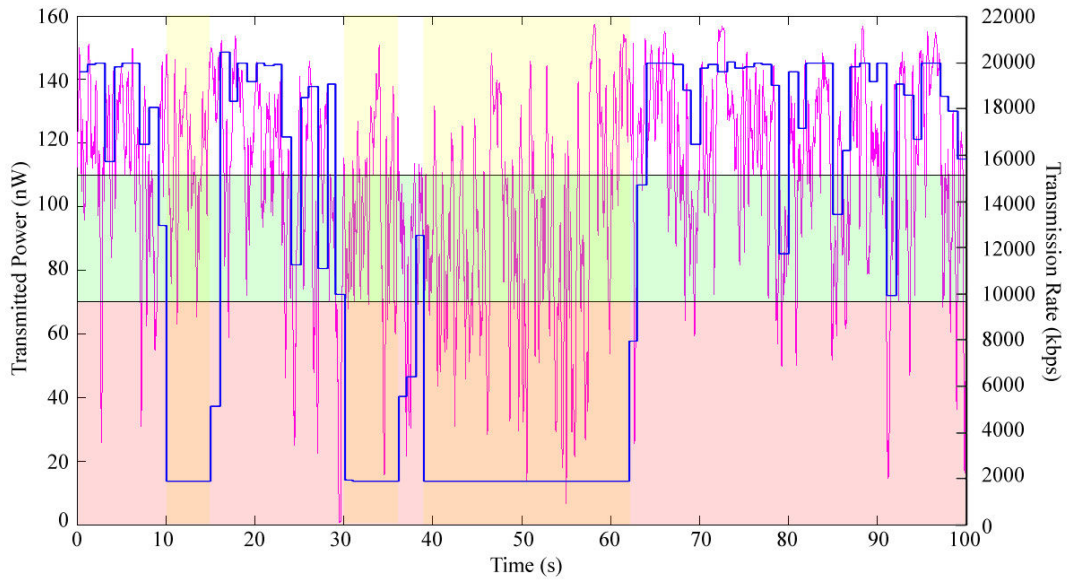


Figure 5-18. Transmission rate for 5 second averaging window.

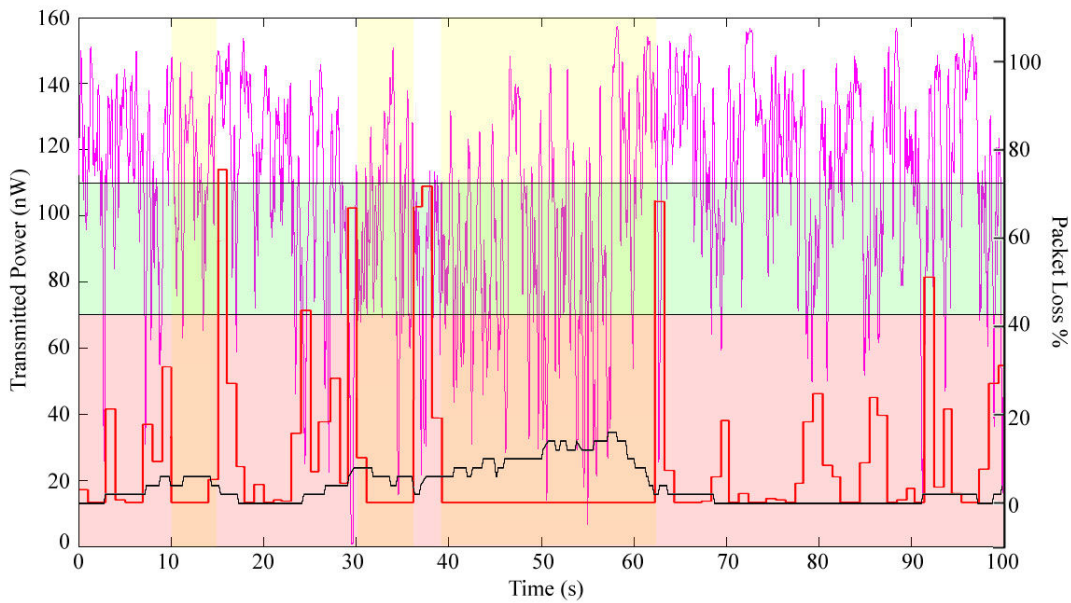


Figure 5-19. Packet loss for 5 second averaging window.

Figures 5-18 and 5-19 show that a 5 second window is quite sensitive to short term drops in link quality. Switching to RF is triggered three times compared to just one in the previous runs. The active link is switched to RF at 10, 30, and 39 second points.

The loss peaked at 16% with a total loss of 26 packets. Using this short a time window makes the system much more susceptible to overly frequent switching. In instances where there are short drops in link quality, switching back and forth between RF and optical may drop the average transmission rate more than necessary to maintain reliability. So far the 10 second and 25 second averaging windows seem the most optimal time intervals for responsive but not too active switching.

5.2.2 Line of Sight Blocking

Lastly, the handling of sudden line of sight blocking was tested for each averaging time window. Each test ran for 60 seconds, where a line of sight blockage was introduced for 20 seconds starting at the 20 second mark until the 40 second mark. This was accomplished by programming the modulator to fully transmit or cut off the light at the proper time. Below is the test for a 50 second averaging window.

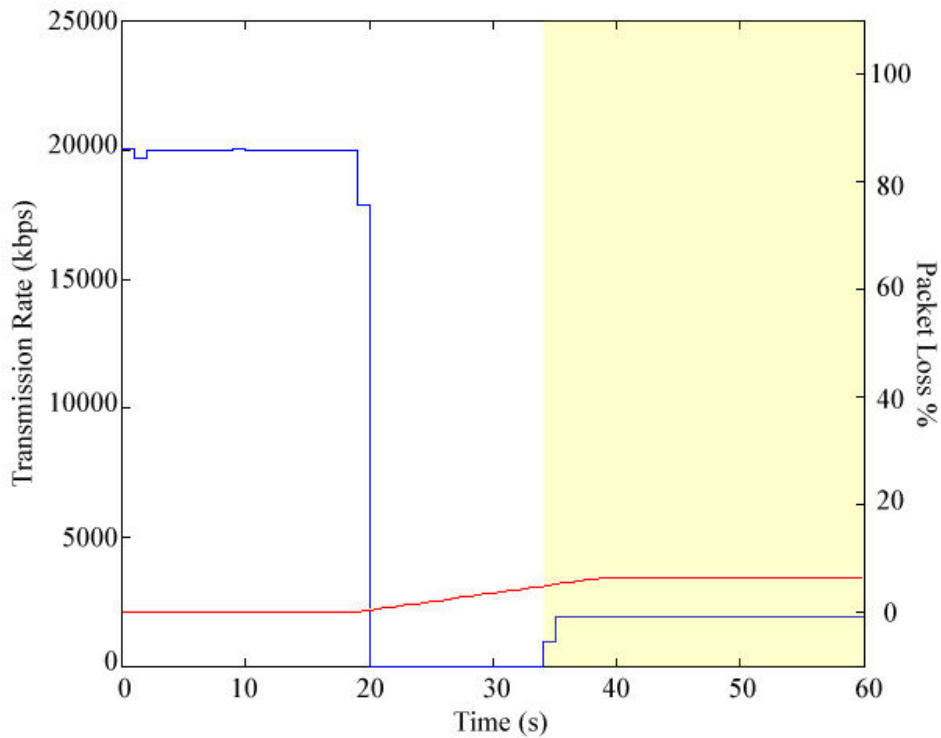


Figure 5-20. Line of sight block test for 50 second window. The blue line represents transmission rate, red is the echo packet loss, and the yellow area represents the time when the RF link is active.

Figure 5-20 shows the line of sight block at 20 seconds. For the 50 second averaging window, the threshold for switching was reached at 34 seconds. Which means there was a total link outage of 14 seconds from the time of blockage until the system was switched to the RF link. Losses peaked at 6.4% when the line of sight blockage was cleared at 40 seconds. Due to the relatively longer averaging time, the optic link was not restored by the program before the end of the 60 second run. Next the test was run again using a 25 second averaging window.

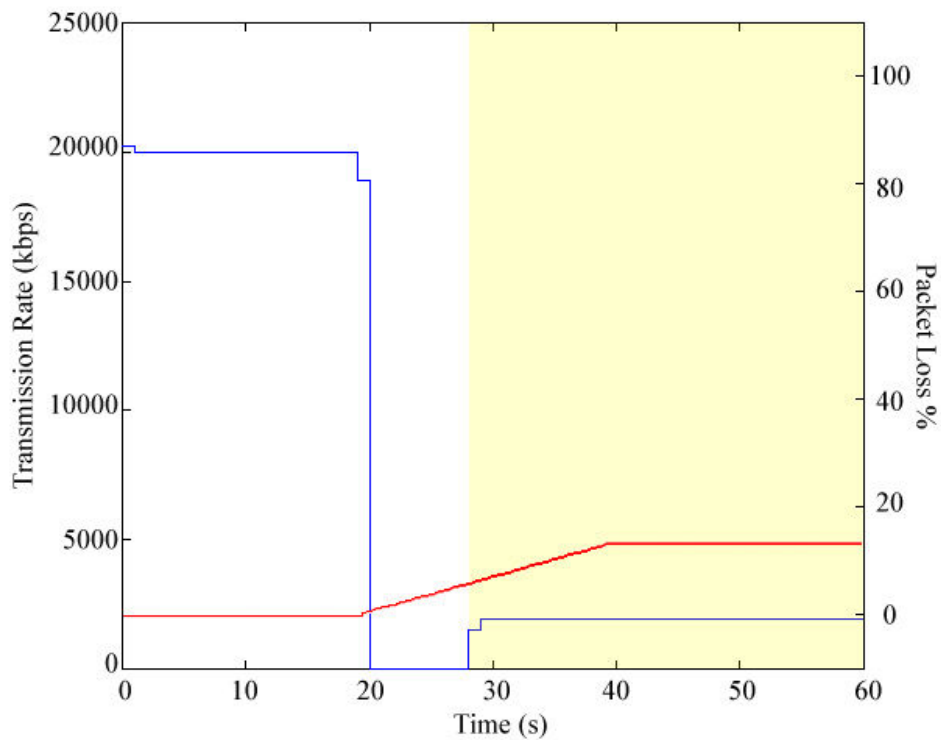


Figure 5-21. Line of sight block test for 25 second window.

The figure above shows a much faster switching time than seen in the 50 second run. The threshold for switching was reached at 27 seconds. Losses peaked at 13.2% at 40 seconds. As one might expect, the total link down time was only 7 seconds, which is half of the 50 second run. Since the averaging window is half as long switching can occur twice as fast. But as in the 50 second run, the optical link was not restored before the end of the test.

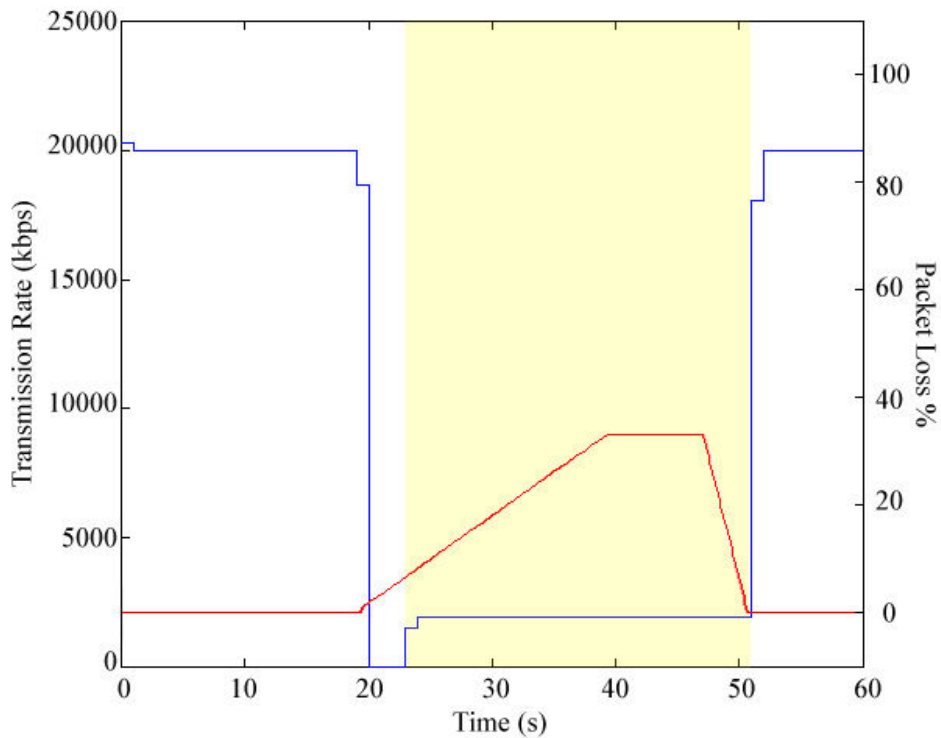


Figure 5-22. Line of sight block test for 10 second window.

The next run made for a 10 second window, is shown above. This time the threshold for switching was reached at 22 seconds, giving only 2 seconds of total link down time before switching to the RF link. Losses peaked at 33% at 40 seconds. This time the averaging window was short enough to restore the optical link within the test runtime. The restoration took about 3 seconds once the loss average number started to come back down. The loss % number can recover much more quickly than lost as easily seen by the slope of the packet loss line. This is due to the fact that when a packet is dropped and times out, there is a minimum wait time for the timeout to occur. This wait time is about 500 ms, therefore a maximum of 2 packets can be lost per second compared to 10 being received with the 100 ms interval of successful pings. This makes recovery of the loss average about 5 times faster than the loss.

But even with this, the total recovery time is limited by the size of the averaging window. Hence it took about 10 seconds, the window size, for the system to switch back to the optical link as seen in Figure 5-22. Once the packet losses stop, enough time needs to pass before the loss average can begin to recover.

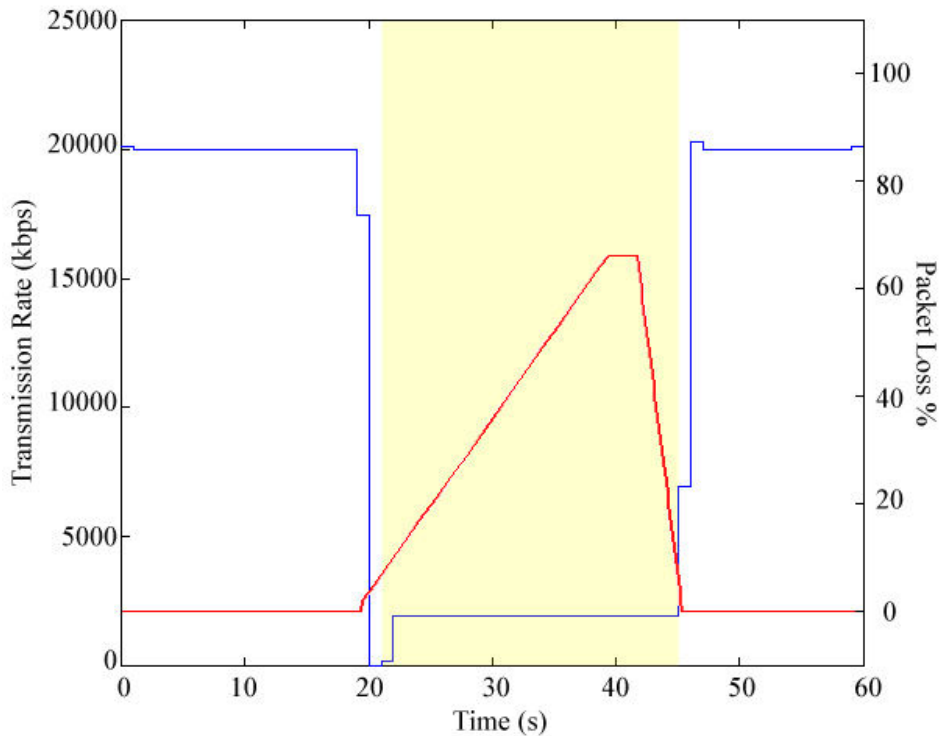


Figure 5-23. Line of sight block test for 5 second window.

The final test was made using a 5 second averaging window. This time the threshold for switching was reached within a second of line of sight blocking. Packet loss peaked at 66% and it only took about 5 seconds for the system to switch back to the optical link once the blockage was cleared. This window size had the fastest reaction time for line of sight blocking of all the tests run. Normally one would think faster is better, but in cases where there are very short intermittent blockages of about a second or two, this window size would cause an excessive amount of flipping back

and forth from optical to RF and back. Also considering other broader effects such as what was tested in 5.2.1, a 5 second window may be too sensitive to momentary drops in optical link quality. The 10 or 25 second windows seem to strike the right balance between having faster reactions and insensitivity to minor drops in link quality. As one might expect, the longer the averaging window the more the system will overlook short term drops in the optical link and shorter the window vice versa. In general these parameters may work well in the conditions tested for in this project; however it does not mean they are well suited for all desired link behaviors or situations.

Chapter 6: Conclusion

In this project, a simple scheme for switching between a RF and optical link in a hybrid system was explored and tested. A fiber optic link was setup to simulate attenuation from atmospheric effects in order to make testing easier and consistent. Most of the critical switching decisions are made during intermittent outages of optical link. Therefore most of the testing was centered on degraded but not completely lost link situations.

Looking at the behavior of the optic link over a range of optical powers, it was apparent that the link is perfectly stable until the power drops below a certain level. Below this level the link quality quickly degrades and then cuts off. This is due to the nature of digital transmission. Once the received power level approaches the decision threshold for determining a 1 or 0 bit, packets will start to get lost as bits are misread and error checking at the lower layers start dropping corrupt packets [30]. This sudden cutoff makes it difficult if not impossible to anticipate when a loss of link will occur. Switching at every instance of link loss may not be the optimal solution especially when the drops are intermittent. In an effort to smooth out the temporary drops, an averaging solution was devised as the simplest means.

For the tests, a method of using a running average of dropped echo packets was used. Echo packets have the advantage of being easy to use, have low overhead, and able to test both transmit and receive sides of a link at once. They can also be in any hardware configuration as long as TCP and IP protocols are supported. One of

the main objectives of testing was to see how different size averaging windows would react to the simulated scintillation.

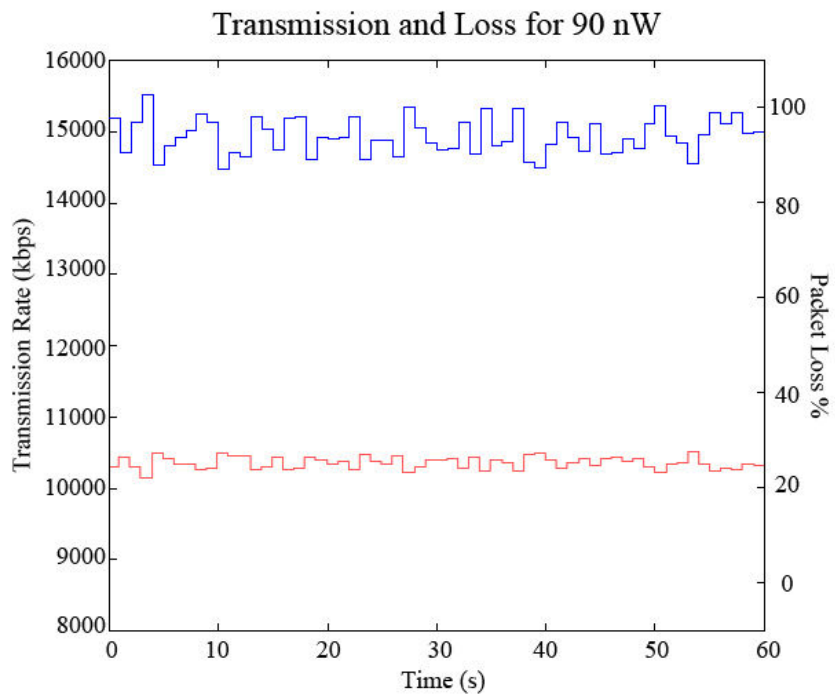
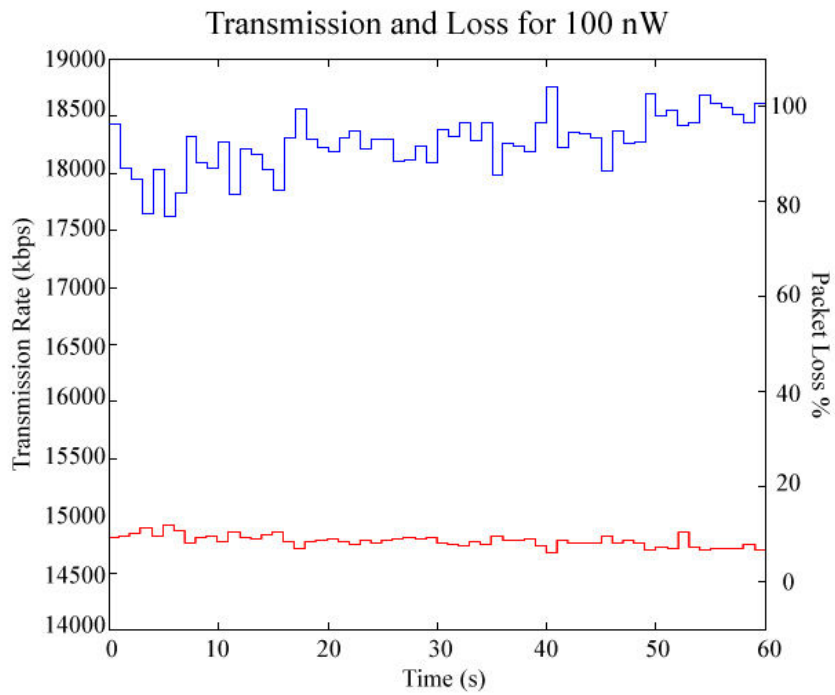
As one may suspect, the different averaging window tests show that with increasing window sizes, the more the scintillation effect is smoothed out and the shorter the size, the more of the effect is “seen”. Therefore there is a tradeoff when picking windows sizes that are either longer or shorter. Longer windows can effectively ignore short term drops in link quality and prevent overly frequent flip-flopping between the RF and optical links but are slow to react to sudden total dropouts such as in line of sight blocks. Shorter windows are quicker to react but are also more prone to unnecessarily excessive switching. In general, routers also have a function to monitoring links using echo packets built-in. However these packets are not tracked in an average and therefore prone to flip-flopping when the optical link goes in and out. In the end, the key is striking a balance between quicker reactions to over sensitivity when choosing the optimal window size, which of course depends on the desired behavior of the system.

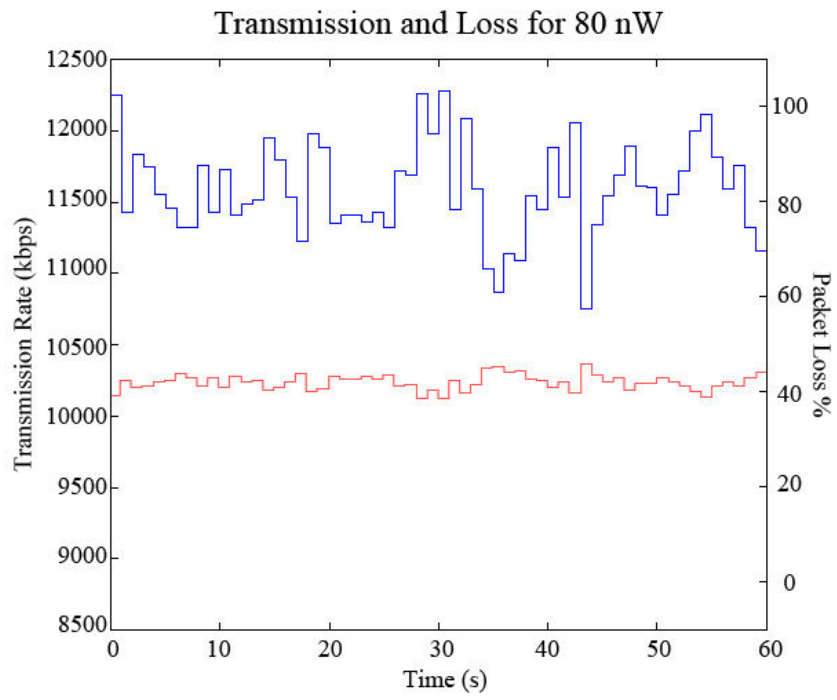
One of the shortcomings of using echo packets as a metric for switching is that it can only react to changes in the link quality and therefore some data will inevitably be lost before a switch can be made to the backup. Since it has no access to Physical Layer data such as received optical power, the system has no way of anticipating a loss in link quality. If Physical Layer data was available and worsening atmospheric conditions were to gradually lower the received optical power, then conceivably the system could be preemptively switched to the backup RF link before any losses were incurred. However, even with such a system sudden line of sight

blocks or rapid changes in weather would not provide enough warning to make preemptive switches. Another feature lacking in this system is that it doesn't maximize the use of the bandwidth available at all times. Such as when both the RF and FSO links are working well, all data is transmitted over the FSO link while the RF remains idle. In situations where security is a concern and RF use is to be minimized, this may not be a bad thing. But in general, the lack of load balancing between the two links is an area where improvements can be made. But as with any system, no system is perfect for all conditions and situations.

Overall, using averaged echo packet losses to make switching decisions was shown to be a simple yet effective means of combining two separate links, backing up one link for the other to improve overall reliability. The system tested does have limitations but in exchange it is simple in design and does not require special equipment or specialized hardware to implement. Future work to improve the system may be done on trying to get more metrics from the link, such as Physical Layer information, to have more information for switching decisions. Also, implementation of load balancing between the two links to maximize data rates and availability would be advantageous for many situations. Such a system could be combined with an error correcting code to further improve performance for some added complexity and latency cost.

Appendix A- Transmission and Loss Graphs for 100, 90, and 80 nW





Appendix B- Matlab Code for Scintillation Data Formatting

```
clear all
close all
directory=['C:\Documents and Settings\Kim\Desktop\Scint data\'];
data=[directory 'tvaldata100Hz100s.txt'];
[time,value]=textread(data,'%f %f');

elmlen=length(value);
maxval=max(value);
minval=min(value);

timelen=100;
sclmax=8;
sclmin=2;
sclwidth=sclmax-sclmin;
sclfactor=sclwidth/(maxval-minval)
sclshift=sclmin-(sclfactor*minval)

fitamp=128.079152509705;
fitoffset=-1.55483086992208;
fitVpi=6.36236696131536;
fitbottom=19.9706085250803;

for n=1:1:elmlen
    adjval(n,1)=(value(n)*sclfactor) + sclshift;
    powerval(n,1)=fitamp*cos((pi*(adjval(n,1)+fitoffset))/
(2*fitVpi))^2 + fitbottom;
end

figure(1);
plot(time,powerval,'m');
xlim([0 timelen]);
xlabel('Time (s)');
ylabel('Transmitted Power (nW)');
hold on
plot(time, 70,'k');
plot(time, 110,'k');
hold off
```

Appendix C- C++ Code for Switching Program

```
//Packet header structures
struct IPHeader {
    unsigned char version:4;
    unsigned char h_len:4;
    unsigned char tos;
    unsigned short total_len;

    unsigned short ident;
    unsigned short flags;

    unsigned char ttl;
    unsigned char proto;
    unsigned short checksum;

    unsigned long source_ip;
    unsigned long dest_ip;
};

struct ICMPHeader {
    unsigned char type;
    unsigned char code;
    unsigned short checksum;
    unsigned short id;
    unsigned short seq;

    unsigned long timestamp;
};

//Main body of program
#include <winsock2.h>
#include <ws2tcpip.h>
#include <winbase.h>
#include <iostream>

#include <shellapi.h>
#include <time.h>
#include <fstream>

#include "packet.h"

#define DEFAULT_IP "192.168.1.2"
#define DEFAULT_PORT 0
#define DEFAULT_PINGINT 100 //Ping interval
#define DEFAULT_SWITCHINT 1000 //Min switching interval
#define DEFAULT_BUFFER 100
#define DEFAULT_TTL 100

using namespace std;

int main()
{
    //Startup Winsock for network socket use.
    WSADATA wsaInfo;
```

```

int errortest = 0;

errortest = WSASStartup(MAKEWORD(2,2), &wsaInfo);
if (errortest != 0) {
    cout <<"WSASStartup Failed. Error code: " <<errortest <<endl;
    return 0;
}
else
    cout <<"WSASStartup successful.\nRunning version: "
<<LOBYTE(wsaInfo.wVersion) <<"." <<HIBYTE(wsaInfo.wVersion) <<endl;

//Create network socket.
SOCKET OpSocket = INVALID_SOCKET;

OpSocket = socket(AF_INET, SOCK_RAW, IPPROTO_ICMP);
if (OpSocket == INVALID_SOCKET) {
    cout <<"Failed to create sockets. Code: "
<<WSAGetLastError() <<endl;
    WSACleanup();
    return 0;
}
else
    cout <<"Socket creation successful.\n";

unsigned long ttl = DEFAULT_TTL;

errortest = setsockopt(OpSocket, SOL_SOCKET, SO_RCVTIMEO, (const
char*)&ttl, sizeof(ttl));
if (errortest == SOCKET_ERROR){
    cout <<"Setsockopt timeout failed.\n";
    WSACleanup();
    return 0;
}

//Create connection for socket.
sockaddr_in outadd;
char *netip;

netip = "192.168.1.2";
outadd.sin_family = AF_INET;
outadd.sin_addr.s_addr = inet_addr(netip);
outadd.sin_port = htons(DEFAULT_PORT);

netip = 0;
errortest = connect(OpSocket, (SOCKADDR*)&outadd,
sizeof(outadd));
if (errortest == SOCKET_ERROR) {
    cout <<"Connection failed.\n";
    closesocket(OpSocket);
    WSACleanup();
    return 0;
}
else
    cout <<"Connection to " <<inet_ntoa(outadd.sin_addr) <<"
successful." <<endl;

//Setup serial port control for router

```

```

        HANDLE SCom;
        DCB dcb;
        OVERLAPPED overlap;
        char cmdbuf[]="\n\n enable\n config t\n router eigrp 1\n",
oncmd[]="network 192.168.1.0\n", offcmd[]="no network
192.168.1.0\n";

        SCom = CreateFile("\\\\.\\COM10", GENERIC_READ | GENERIC_WRITE,
0, NULL, OPEN_EXISTING, FILE_ATTRIBUTE_NORMAL, NULL);
        if (SCom == INVALID_HANDLE_VALUE){
            cout <<"Serial connection failed.\n";
            return 0;
        }
        else
            cout <<"Serial connection success. Handle created.\n";

        if (GetCommState(SCom, &dcb) == 0){
            cout <<"GetCommState failed.\n";
            CloseHandle(SCom);
            return 0;
        }
        else
            cout <<"GetCommState success.\n";

        if (BuildCommDCB("baud=9600 parity=N data=8 stop=1",&dcb) == 0){
            cout <<"Failed to Build DCB. Error: " <<GetLastError()
<<endl;
            CloseHandle(SCom);
            return 0;
        }
        else
            cout <<"BuildComm success.\n";

        if (SetCommState(SCom, &dcb) == 0){
            cout <<"SetCommState failed.\n";
            CloseHandle(SCom);
            return 0;
        }
        else
            cout <<"SetCommState success.\n";

//Take user input for switching parameters
        unsigned long delay = DEFAULT_PINGINT, sumwindow = 0, runtime =
0, sumlen = 0, hiqual = 100, loqual = 0;
        cout <<"Input run time (seconds): ";
        cin >>runtime;
        if (runtime < 0){
            cout <<"Run time must be non-negative.\n";
            return 0;
        }
        runtime = runtime * 1000; //Run time of 0 is endless run

        cout <<"Input avg sum window (seconds): ";
        cin >>sumwindow;
        if (sumwindow <= 0){
            cout <<"Window must be greater than 0.\n";
            return 0;
        }

```

```

    }
    sumlen = (unsigned long)((float)1000/delay * sumwindow);

    cout <<"Input lower packet success rate %: ";
    cin >>loqual;

    cout <<"Input upper packet success rate %: ";
    cin >>hiqual;

//Setup timing system for ping timing and output log file
    float avg, rntime, avgchk;
    unsigned long starttime = GetTickCount(), switchint = 0, avgsum
= sumlen, sumchk;
    unsigned short runsum[sumlen], indx = 0, multi = 1, swch = 0,
pktsent = 0, tmoutcnt = 0, misscnt = 0;
    clock_t dlycnt;

    ofstream outfile ("echolog.txt");
    outfile <<"100\t0\n";

    for (int cnt = 0; cnt < sumlen; cnt++)
        runsum[cnt] = 1;

//Packet send/receive header prep
    sockaddr_in recvadd;
    int pktsize = sizeof(ICMPHeader), chksize, data_in, recvsz =
sizeof(recvadd);
    unsigned short seqno = 1, *chkpkt;
    unsigned long chksum;
    ICMPHeader pkthead, *icmppkt, *icmprecv;
    IPHeader *recvbuf = (IPHeader*)new char[DEFAULT_BUFFER];

    icmppkt = &pkthead;

    icmppkt->type = 8; //Echo request
    icmppkt->code = 0;
    icmppkt->checksum = 0;
    icmppkt->id = (unsigned short)GetCurrentProcessId(); //Process
id converted from ulong->ushort

    icmprecv = (ICMPHeader*)((char*)recvbuf + 20); //Skip IP header
and mark beginning of ICMP header

//Packet loop
while(1){
    icmppkt->checksum = 0;
    icmppkt->seq = seqno;
    icmppkt->timestamp = GetTickCount(); //Milliseconds since system
startup

//Calculate checksum for packet header
    chksize = pktsize;
    chksum = 0;
    chkpkt = (unsigned short*)icmppkt;

    while (chksize > 1){ //Add all the words together
        chksum += *chkpkt++;
    }
}

```

```

        chksize -= 2;
    }
    if (chksize == 1) //Add final odd byte
        chksum += *(unsigned char*)chkpkt;

    chksum = (chksum >> 16) + (chksum & 0xffff); //Add high 16 to
low 16
    chksum += (chksum >> 16); //Add carry

    icmppkt->checksum = (unsigned short)(~chksum); //Truncate to 2
bytes

//Send packet
    errortest = send(OpSocket, (char*)icmppkt, pktsize, 0);
    if (errortest == SOCKET_ERROR){
        cout <<"Send packet failed. Code: " <<WSAGetLastError()
<<endl;
        closesocket(OpSocket);
        WSACleanup();
        return 0;
    }
    else
        pktsent++;

    rntime = (float)((GetTickCount() - starttime) / 1000;
    dlycnt = clock() + delay;

//Receive reply
    errortest = 0;
reread:
    data_in = 0;
    data_in = recvfrom(OpSocket, (char*)recvbuf, DEFAULT_BUFFER, 0,
(sockaddr*)&recvadd, &recvsz);

if (data_in == SOCKET_ERROR && WSAGetLastError() != 10060){
    cout <<"Read failed, ";
    if (WSAGetLastError() == WSAEMSGSIZE)
        cout <<"buffer too small.\n";
    else
        cout <<"error: " <<WSAGetLastError() <<endl;
    closesocket(OpSocket);
    WSACleanup();
    return 0;
}

if (WSAGetLastError() == 10060){
    cout <<"Read failed, timed out.\n";
    errortest = 1;
    ttimeoutcnt++;
    goto skip;
}

//Reply check
    if (icmprecv->type != 0 || icmprecv->code != 0){
        cout <<"Echo type mismatch= " <<icmprecv->type <<endl;
        cout <<"Echo code mismatch= " <<icmprecv->code <<endl;
        goto reread;
    }

```



```

    }

    if (icmprecv->id != icmppkt->id){
        cout <<"Id mismatch= " <<icmprecv->id <<endl;
        goto reread;
    }

    if (icmprecv->seq != seqno){
        cout <<"Sequence number mismatch= " <<seqno <<"-"<<endl;
        errorrest = 1;
    }

    if (icmprecv->checksum != icmppkt->checksum + 8){
        cout <<"Checksum mismatch= " <<icmppkt->checksum <<"-"<<endl;
        errorrest = 1;
    }

    if (errorrest == 1)
        misscnt++;

skip:
    if (seqno < 65500)
        seqno++;
    else
        seqno = 1;

//Average window tracking and switching decision
    avgsum -= runsum[indx];
    if (errorrest == 1)
        runsum[indx] = 0;
    else
        runsum[indx] = 1;
    avgsum += runsum[indx];
    indx++;
    if (indx >= sumlen)
        indx = 0;

    avg = ((float)avgsum / (float)sumlen) * 100;
    if (avg <= loqual && swch == 0 && switchint <= GetTickCount()){
        WriteFile(SCom,offcmd,strlen(offcmd),NULL,&overlap);
        cout <<"Quality low, switching to RF.\n\n";
        switchint = GetTickCount() + DEFAULT_SWITCHINT;
        swch = 1;
    }
    if (avg >= hiqual && swch == 1 && switchint <= GetTickCount()){
        WriteFile(SCom,oncmd,strlen(oncmd),NULL,&overlap);
        cout <<"Quality good, switching to FSO.\n\n";
        switchint = GetTickCount() + DEFAULT_SWITCHINT;
        swch = 0;
    }

//Save average and time to log file
    outfile <<avg <<"\t" <<rntime <<"\n";
    cout <<"Avg: " <<avg <<" Avgsum: " <<avgsum <<" Time: " <<rntime
<<endl;

```

```

//Double check if running average is accurate
    if (GetTickCount() > starttime + (multi * sumwindow * 1000)){
        sumchk = 0;
        for (int cnt = 0; cnt < sumlen; cnt++){
            sumchk += runsum[cnt];
            avgchk = ((float)sumchk / (float)sumlen) * 100;
            if (avgchk != avg){
                avg = avgchk;
                cout <<"Avg mismatch: " <<avg <<"-" <<avgchk <<endl;
            }
            multi++;
        }
}

//Display total statistics of run
    if ((GetTickCount() > starttime + runtime || GetTickCount() <
starttime) && runtime != 0){

        cout <<"Total pings sent: " <<pktsent <<endl;
        cout <<"Total packets timedout: " <<tmoutcnt <<endl;
        cout <<"Total mismatched: " <<misscnt <<endl;

        delete[] recvbuf;
        closesocket(OpSocket);
        WSACleanup();
        return 1;
    }

    if (delay != 0){
        while (dlycnt > clock()){}
    }
}

    closesocket(OpSocket);
    CloseHandle(SCom);
    WSACleanup();
    return 1;
}

```

Bibliography

- [1] Cordeiro, M.C.R., Colvero, C.P., von der Weid, J.P., "Experimental comparison of scintillation effects in far and near infrared wavelengths in FSO systems," *International Conference on Microwave and Optoelectronics*, pp. 393-395, July 2005.
- [2] Mahdy, A.M., Deogun, J.S., "Optimizing Free Space Optics for City-Wide Wireless Networks," *International Conference on Networking*, p. 66, April 2007.
- [3] Alma, H., Al-Khateeb, W., "Effect of weather conditions on quality of Free Space Optics links (with focus on Malaysia)," *International Conference on Computer and Communication Engineering*, pp. 1206-1210, May 2008.
- [4] Leitgeb, E., Bregenzer, J., Fasser, P., Gebhart, M., "Free space optics - extension to fiber-networks for the "last mile"," *IEEE Lasers and Electro-Optics Society*, vol. 2, pp. 459-460, Nov. 2002.
- [5] Yoshida, K., Tsujimura, T., Shiraki, K., Sankawa, I., "A free space optics system for seamless transmission between single-mode optical fibers," *SICE*, pp. 2333-2336, Sept. 2007.
- [6] Muhammad, S. Sheikh, Kamalakis, T., Leitgeb, E., Koudelka, O., Kandus, G., Javornik, T., "Terrestrial Free Space Optical Links for High Bandwidth Connectivity," *IEEE International Multitopic Conference*, pp. 1-5, Dec. 2005.
- [7] Izadpanah, H., ElBatt, T., Kukshya, V., Dolezal, F., Ryu, B.K., "High-availability free space optical and RF hybrid wireless networks," *IEEE Wireless Communications*, vol. 10, pp. 45-53, April 2003.
- [8] Kim, I.I., Korevaar, E.J., "Availability of Free Space Optics (FSO) and hybrid FSO/RF systems," *Proc. SPIE*, vol. 4530, pp. 84-95, 2001.
- [9] Sizun, H., *Radio Wave Propagation for Telecommunication Applications*. Paris: Springer, 2005.
- [10] Kukshva, V., Rappaport, T.S., Izadpanah, H., Tangonan, G., Guerrero, R.A., Mendoza, J.K., Lee, B., "Free-space optics and high-speed RF for next generation networks - Propagation Measurements," *IEEE Vehicular Technology Conference*, vol. 1, pp. 24-28, Sept. 2002.
- [11] Chartrand, M.R., *Satellite Communications for the Nonspecialist*. Bellingham: SPIE Press, 2004.

- [12] Andrews, L.C., Phillips, R.L., Hopen, C.Y., *Laser Beam Scintillation with Applications*. Bellingham: SPIE Press, 2001.
- [13] Willebrand, H., Ghuman, B.S., *Free-Space Optics: Enabling Optical Connectivity in Today's Networks*. Indianapolis: Sams Publishing, 2002.
- [14] Kamalakis, T., Neokosmidis, I., Tsipouras, A., Pantazis, S., Andrikopoulos, I., "Hybrid Free Space Optical / Millimeter Wave Outdoor Links for Broadband Wireless Access Networks," *IEEE International Symposium on Personal, Indoor and Mobile Radio Communications*, pp. 1-5, Sept. 2007.
- [15] Shaw, J., "Introduction to Optical Remote Sensing Systems," *SPIE Short Courses*, Aug. 2008.
- [16] Kavehrad, M., Hamzeh, B., "Laser communication system using wavelet-based multi-rate signaling," *Military Communications Conference*, vol. 1, pp. 398-403, Nov 2005.
- [17] Chen, E.F., "Temperature Mapping of an Acoustically Forced Laminar Diffusion Flame Using Planar Laser Rayleigh Scattering," Masters thesis, University of Maryland, 2005.
- [18] Friedlander, S.K., *Smoke, Dust, and Haze: Fundamentals of Aerosol Dynamics*. New York: Oxford University Press, 2000.
- [19] Jackson, J.D., *Classical Electrodynamics*, 3rd ed. Hoboken: John Wiley & Sons, Inc., 1999.
- [20] Nadeem, F., Flecker, B., Leitgeb, E., Khan, M.S., Awan, M.S., Javornik, T., "Comparing the fog effects on hybrid network using optical wireless and GHz links," *International Symposium on Communication Systems, Networks and Digital Signal Processing*, pp. 278-282, July 2008.
- [21] Tyson, R.K., *Introduction to Adaptive Optics*. Bellingham: SPIE Press, 2000.
- [22] Yuksel, H., Davis, C.C., "Aperture averaging experiment for optimizing receiver design and analyzing turbulence on free space optical communication links," *Conference on Lasers and Electro-Optics*, vol. 1, pp. 743-745, May 2005.
- [23] Kozierok, C.M., *The TCP/IP Guide: A Comprehensive, Illustrated Internet Protocols Reference*. San Francisco: No Starch Press, Inc., 2005.
- [24] Spurgeon, C.E., *Ethernet: The Definitive Guide*. Sebastopol: O'Reilly & Associates, Inc., 2000.

- [25] Vangala, S., Pishro-Nik, H., "Optimal Hybrid RF-Wireless Optical Communication for Maximum Efficiency and Reliability," *CISS*, March 2007.
- [26] Goldsmith, A., *Wireless Communications*. New York: Cambridge University Press, 2005.
- [27] Protocol Engineering Advanced Networking Research Group, *Networks and Communications Systems Branch*: <<http://cs.itd.nrl.navy.mil/work/mgen/>>, 2008.
- [28] Iga, K., Kokubun, Y., *Encyclopedic handbook of integrated optics*. Boca Raton: CRC Press, 2006.
- [29] Cvijetic, M., *Optical Transmission Systems Engineering*. Norwood: Artech House, 2004.
- [30] Agrawal, G.P., *Fiber-optic Communication Systems*, 3rd ed. Hoboken: Wiley-Interscience, 2002.